Beam End Repair for Prestressed Concrete Beams

Final Report
September 2020

BRIDGE ENGINEERING CENTER

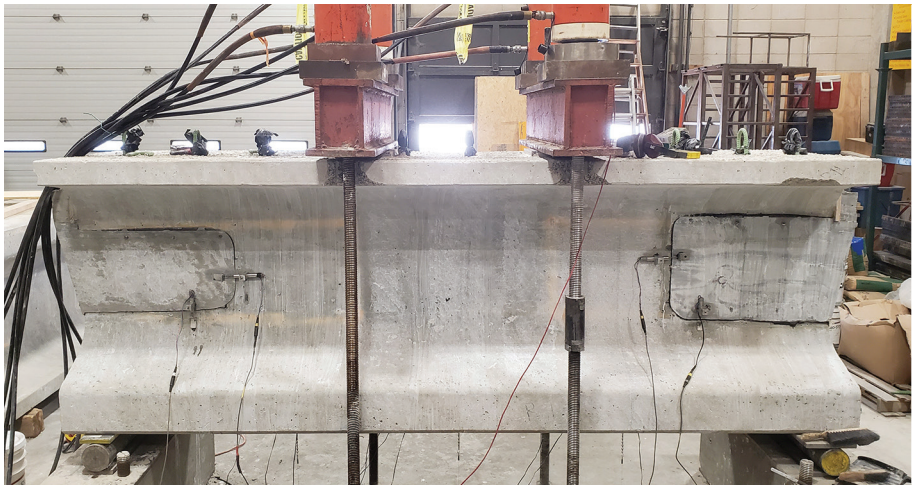

IOWA STATE UNIVERSITY
Institute for Transportation

Sponsored by
Iowa Highway Research Board
(IHRB Project TR-715)
Iowa Department of Transportation
(InTrans Project 17-598)

About the Bridge Engineering Center

The mission of the Bridge Engineering Center (BEC) is to conduct research on bridge technologies to help bridge designers/owners design, build, and maintain long-lasting bridges.

About the Institute for Transportation

The mission of the Institute for Transportation (InTrans) at Iowa State University is to develop and implement innovative methods, materials, and technologies for improving transportation efficiency, safety, reliability, and sustainability while improving the learning environment of students, faculty, and staff in transportation-related fields.

Iowa State University Nondiscrimination Statement

Iowa State University does not discriminate on the basis of race, color, age, ethnicity, religion, national origin, pregnancy, sexual orientation, gender identity, genetic information, sex, marital status, disability, or status as a US veteran. Inquiries regarding nondiscrimination policies may be directed to the Office of Equal Opportunity, 3410 Beardshear Hall, 515 Morrill Road, Ames, Iowa 50011, telephone: 515-294-7612, hotline: 515-294-1222, email: eooffice@iastate.edu.

Disclaimer Notice

The contents of this report reflect the views of the authors, who are responsible for the facts and the accuracy of the information presented herein. The opinions, findings and conclusions expressed in this publication are those of the authors and not necessarily those of the sponsors.

The sponsors assume no liability for the contents or use of the information contained in this document. This report does not constitute a standard, specification, or regulation.

The sponsors do not endorse products or manufacturers. Trademarks or manufacturers' names appear in this report only because they are considered essential to the objective of the document.

Iowa DOT Statements

Federal and state laws prohibit employment and/or public accommodation discrimination on the basis of age, color, creed, disability, gender identity, national origin, pregnancy, race, religion, sex, sexual orientation or veteran's status. If you believe you have been discriminated against, please contact the Iowa Civil Rights Commission at 800-457-4416 or Iowa Department of Transportation's affirmative action officer. If you need accommodations because of a disability to access the Iowa Department of Transportation's services, contact the agency's affirmative action officer at 800-262-0003.

The preparation of this report was financed in part through funds provided by the Iowa Department of Transportation through its "Second Revised Agreement for the Management of Research Conducted by Iowa State University for the Iowa Department of Transportation" and its amendments.

The opinions, findings, and conclusions expressed in this publication are those of the authors and not necessarily those of the Iowa Department of Transportation.

1. Report No.	2. Government Accession No.	3. Recipient's Catalog No.
IHRB Project TR-715		

4. Title	5. Report Date
Beam End Repair for Prestressed Concrete Beams	September 2020
	6. Performing Organization Code

7. Authors	8. Performing Organization Report No.
Behrouz Shafei (orcid.org/0000-0001-5677-6324), Brent Phares (orcid.org/0000-0001-5894-4774), and Weizhuo Shi (orcid.org/0000-0001-8193-0098)	InTrans Project 17-598

9. Performing Organization Name and Address	10. Work Unit No. (TRAIS)
Bridge Engineering Center Iowa State University 2711 South Loop Drive, Suite 4700 Ames, IA 50010-8664	11. Contract or Grant No.

12. Sponsoring Organization Name and Address	13. Type of Report and Period Covered
Iowa Highway Research Program Iowa Department of Transportation 800 Lincoln Way Ames, IA 50010	Final Report
	14. Sponsoring Agency Code

15. Supplementary Notes

Visit https://intrans.iastate.edu for color pdfs of this and other research reports.

16. Abstract

One of the primary concerns of the use of precast prestressed concrete beam (PPCB) bridges is cracking and spalling of the concrete towards the ends of the beams due to contamination from water and deicing chemicals, which results in exposure and corrosion of the beams' reinforcement and prestressing strands. If allowed to progress, this deterioration will compromise the capacity of the beams, which can affect the integrity of the entire bridge and raise safety and durability concerns.

To address this issue, the efficacy of ultra-high performance concrete (UHPC) and high early strength concrete (HESC) for strengthening and repairing damaged prestressed concrete beams ends was evaluated. First, a review of current repair strategies was conducted to determine the key qualities of effective repair methods. The use of unique materials with enhanced properties to perform patch repairs was ultimately selected as the repair method evaluated in this research project. Small-scale laboratory testing was conducted to evaluate the bond strength of various potential patching materials in terms of shear stress and tensile stress. Full-scale laboratory testing was conducted to determine the properties and performance of UHPC and HESC as beam patching materials. Six artificially damaged prestressed concrete beams were tested in full-scale experiments: two without repair, two repaired with UHPC, and two repaired with HESC.

Observations indicated excellent patch bonding by the two materials tested in the full-scale portion of this research. Failure of one of the unrepaired beams due to confinement failure demonstrated one consequence of the loss of concrete cover and damage to the reinforcing steel caused by the beam-end damage. The outcome of this study is a set of recommendations regarding the most effective repair methods and appropriate retrofit materials for rehabilitating prestressed concrete beam ends.

17. Key Words	18. Distribution Statement
beam end patching—bond strength—bridge girder repairs—high early strength concrete—prestressed concrete bridges—shear strength—shrinkage compensating cement concrete—ultra-high performance concrete	No restrictions.

19. Security Classification (of this report)	20. Security Classification (of this page)	21. No. of Pages	22. Price
Unclassified.	Unclassified.	72	NA

BEAM END REPAIR FOR PRESTRESSED CONCRETE BEAMS

Final Report
September 2020

Principal Investigator
Behrouz Shafei, Associate Professor
Bridge Engineering Center, Iowa State University

Co-Principal Investigator
Brent M. Phares, Research Associate Professor
Bridge Engineering Center, Iowa State University

Research Assistant
Quin Rogers

Authors
Behrouz Shafei, Brent M. Phares, and Weizhuo Shi

Sponsored by
Iowa Highway Research Board and
Iowa Department of Transportation
(IHRB Project TR-715)

Preparation of this report was financed in part
through funds provided by the Iowa Department of Transportation
through its Research Management Agreement with the
Institute for Transportation
(InTrans Project 17-598)

A report from
Bridge Engineering Center
Iowa State University
2711 South Loop Drive, Suite 4700
Ames, IA 50010-8664
Phone: 515-294-8103 / Fax: 515-294-0467
https://intrans.iastate.edu

TABLE OF CONTENTS

LIST OF FIGURES

LIST OF TABLES

ACKNOWLEDGEMENTS

The authors would like to acknowledge the Iowa Highway Research Program (IHRB) and Iowa Department of Transportation (DOT) for sponsoring this project.

Special thanks are due to Ahmad Abu-Hawash, Dean Bierwagen, and Wayne Sunday of the Iowa DOT for their participation in the technical advisory committee (TAC). Additionally, the authors would like to recognize Doug Wood, manager of the Structural Engineering Research Laboratory at Iowa State University (ISU), for his assistance with laboratory testing, Owen Steffens at ISU for his assistance with specimen preparation and testing, and undergraduate student Eric Lezniak and other laboratory assistants for their assistance with specimen preparation.

Special thanks are also due to Forterra Pipe & Precast for its generous donation of the prestressed beam specimen used in laboratory testing for this investigation.

EXECUTIVE SUMMARY

One of the primary concerns with the use of precast prestressed concrete beam (PPCB) bridges is cracking and spalling of the concrete towards the ends of the beams due to contamination from water and deicing chemicals, which results in exposure and corrosion of the beams' reinforcement and prestressing strands. If allowed to progress, this deterioration will compromise the capacity of the beams, which can affect the integrity of the entire bridge and raise safety and durability concerns.

In order to address this issue, the efficacy of ultra-high performance concrete (UHPC) and high early strength concrete (HESC) for strengthening and repairing damaged prestressed concrete beam ends was evaluated. First, a review of current repair strategies was conducted to determine the key qualities of effective repair methods. The use of unique materials with enhanced properties to perform patch repairs was ultimately selected as the repair method evaluated in this research project. Small-scale laboratory testing was conducted to evaluate the bond strength of various potential patching materials in terms of shear stress and tensile stress. Full-scale laboratory testing was conducted to determine the properties and performance of UHPC and HESC as beam patching materials. Six artificially damaged prestressed concrete beams were tested in full-scale experiments: two without repair, two repaired with UHPC, and two repaired with HESC.

Observations indicated excellent patch bonding by the two materials tested in the full-scale portion of this research. Failure of one of the unrepaired beams due to confinement failure demonstrated one consequence of the loss of concrete cover and damage to the reinforcing steel caused by the beam-end damage. The outcome of this study is a set of recommendations regarding the most effective repair methods and appropriate retrofit materials for rehabilitating prestressed concrete beam ends.

The following key findings resulted from this study:

- Small-scale bond testing for this project consisted of testing four different materials to determine their bonding properties and their suitability for use as patch repair materials. The materials tested included proprietary and nonproprietary UHPC, HESC, and shrinkage compensating cement concrete (SCC-C). Each material was tested under tensile stresses and shear stresses using the splitting tensile strength test and the slant shear strength test, respectively.

- All material types demonstrated good tensile bond strength. The interface surface condition did not demonstrate a significant effect on tensile bond strength for the tested samples. Both the HESC and SCC-C bonded samples exhibited a tensile bond strength comparable to the tensile strength of the plain (unbonded) samples tested. Both types of UHPC samples resulted in higher peak loads resisted. However, for all specimens, the substrate concrete failed before the testing machine reached peak load. Therefore, maximum tensile bond stress could not be determined.

- All material types demonstrated good shear bond strength. No bond failures were observed during slant shear testing. In the case of the HESC and SCC-C samples, failure initiated in the substrate concrete and cracking propagated as vertical splitting cracks in nearly all specimens. Pure substrate failure occurred for the UHPC samples. Some cracks penetrated the UHPC but were mitigated by the steel fibers in the mix. These results suggest that all materials provide adequate bond strength and are suitable for use as patch repair materials.

- Upon completion of the structural tests, all of the repaired specimens maintained their integrity and performance with no failure. There were no significant differences observed in behavior under shear loading among the four patch-repaired girders in the large-scale study.

- Failure of one of the unrepaired beams due to confinement failure demonstrated one consequence of the loss of concrete cover caused by beam-end damage. Both the UHPC and HESC patches demonstrated good bonding to the beam substrate during full-scale testing. Patch repairs are significantly less expensive than beam replacement and are considered to be conventional bridge repairs.

- The beams with patch repairs experienced lower maximum strains and deflections despite being subject to a greater maximum load, indicating that the patching exhibited good bond behavior during loading and unloading. It was found that the amount of shear reinforcement affects beam behavior.

- Further research on the practical aspects and strength-enhancing capabilities of UHPC and HESC for beam-end repair in shear-critical regions is recommended through field investigations.

INTRODUCTION

Background

The use of precast prestressed concrete beam (PPCB) bridges continues to increase as prestressed technology becomes more popular among engineers. Now, more than 60% of newly constructed bridges are built using prestressed concrete girders. One of the effects of prestressing, through mechanisms such as strand wicking action, is the formation of cracks at the beam ends. Although typically small, the cracks allow the beam to be contaminated by water and deicing chemicals, resulting in accelerated concrete deterioration. In the United States, a large number of bridges were built in the 1950s, 1960s, and 1970s, before sealing beam ends became standard. The result is that a growing portion of those bridges are in need of replacement, rehabilitation, or repair. States in the Northeast and Midwest experience harsh climates that further contribute to the deterioration of such bridges.

When possible, expansion joints are eliminated by utilizing integral abutments. However, in cases where integral abutments are not feasible, a common problem noted by departments of transportation (DOTs) across the nation is the considerable deterioration of the beam-end regions compared to the otherwise satisfactory condition of the remainder of the beam. This deterioration has a few contributing factors. Due to failure at the expansion joints, water containing deicing agents begins to flow directly onto the beam ends. Subsequently, freezing and thawing cycles of these saturated beam ends cause scaling and spalling of the concrete cover, resulting in direct exposure of the reinforcing steel. Once the steel is exposed, the girders experience accelerated corrosion and further damage in the region of the water infiltration (Figure 1.1).

Figure 1.1. Severely corroded prestressed concrete girder (Minnesota)

Additional corrosion of the bottom flanges of beam ends results from the chloride-laden runoff near the deck drainage pipes. This type of damage is localized near the bearings and therefore the

principal concern is stress induced in shear. Extensive damage to the girders can result in the loss of ultimate strength, thereby increasing the risk of failure.

Research Objective and Scope

To address the issue of beam-end deterioration, this project investigated innovative solutions for the repair and retrofit of prestressed concrete beam ends (that have been damaged over time) that can restore the full capacity of the beam. Ultimately, the goal was to extend the service life of PPCB bridges. Special effort was also placed on identifying applicable retrofit concepts. This project involved both small-scale and full-scale testing to achieve the following objectives:

1. Identify promising alternative materials to use in place of plain concrete or mortar for patching repairs
2. Evaluate the bond performance of the alternative patching materials identified
3. Determine the efficacy of patch repairs on prestressed concrete beam specimens with simulated beam-end damage in the shear-critical region
4. Restore shear capacity and extend the service life of damaged prestressed beam ends

Report Organization

The first chapter of this report consists of the introduction, background, and research objectives and scope. The second chapter provides a review of the literature related to PPCB bridge repair and rehabilitation. The third and fourth chapters detail the laboratory testing of the small-scale and full-scale specimens, respectively, and present the results of the experimental studies. Finally, the fifth chapter presents the conclusions and recommendations stemming from this research.

LITERATURE REVIEW

Introduction

The ongoing desire for stronger, more efficient, and longer lasting structures has resulted in PPCB bridges becoming popular among engineers. Since their first application in the United States in 1949, prestressed concrete bridges have accounted for a significant percentage of all bridges built in the US, approximately 22% within the last decade (Wu and Chase 2010). The benefits of using prestressed technology in bridge beams include reduced deflections, greater quality control, and reduced construction costs. Different methods of prestressing concrete exist, with the most common being pretensioning and posttensioning. A pretensioned beam is formed by hydraulically tensioning steel strands positioned inside an empty casting bed and pouring concrete around the strands. When the concrete is fully cured, the strands are released, introducing compression into the beam. Posttensioned beams utilize the same principle, but the beam is cast with hollow channels and steel strands are later run through these channels and tensioned against a beam end (Nawy 2010).

In both cases, the transfer of the prestressing forces from the steel strands to the concrete causes large stresses in the beam, particularly at the ends. These high stresses often lead to the formation of cracks in the beam ends (Tadros et al. 2010). Proper steel reinforcement design can keep these cracks below an acceptable width; however, the cracks still allow for the penetration of water and chlorides into the beam ends (Kannel et al. 1997). Cracked beam ends vulnerable to moisture are particularly a problem when located under leaking expansion joints. The use of integral abutments remedies this issue by eliminating expansion joints; however, the problem persists in bridges with non-integral abutments (Ohio DOT 2007). The ingress of contaminants like water and chlorides causes the steel rebar to corrode and produce rust. Although the high pH of the surrounding concrete creates a passive layer around the steel that practically eliminates corrosion, a high concentration of chloride within the concrete destroys this layer, allowing the steel to corrode. The introduction of chloride is particularly an issue in freeze-thaw climates, where deicing salts are often used on roadways.

There are two primary ways in which the ingress of water and chlorides and the subsequent corrosion adversely affect PPCB bridges. The first detrimental effect to occur is a loss of prestressing force due to a reduction in prestressing strand area (Kim et al. 2016). As the steel strands corrode, iron atoms are oxidized, and the resulting positively charged iron ions react with negatively charged hydroxide ions to form rust. On a larger scale, the outer layers of the steel strands are converted to rust, which reduces the cross-sectional area of the steel. This reduction results in a loss of prestressing force, which lessens the benefits of a prestressed beam, such as high capacity and reduced deflections. The second negative effect of water and chloride infiltration takes place after the prestressing strands have undergone fairly substantial corrosion. Because rust occupies a larger volume than the original steel, corrosion causes the strands to effectively expand and exert tensile stresses on the surrounding concrete. Concrete develops cracks relatively easily under these tensile stresses, which can lead to delamination and spalling at the beam ends. Spalling beam ends present a significant safety hazard. Deteriorated beam ends offer a reduced bearing area, therefore lowering the capacity of the beam (Hosteng et al. 2015).

Additionally, spalling of the concrete further exposes prestressing strands and reinforcing steel to the atmosphere, allowing corrosion to occur at a faster rate. Spalled concrete may be patched, but such patches are often not a long-term solution because corrosion continues in the underlying steel (Clemena and Jackson 2000).

Review of Corrosion in Prestressing Steel

As alluded to in the introduction to this chapter, the natural alkalinity of concrete paired with sufficient cover protects the embedded steel against the process of corrosion. Consequently, in order to protect a concrete beam from corrosion damage it is important to understand exactly how corrosion is able to begin in the first place.

Formation of Cracks

The first step in the corrosion of embedded prestressing steel is the formation of cracks in the beam ends. Cracks need not be structurally significant or even very large to create the potential for corrosion of the prestressing steel. In pretensioned girders, cracks generally appear at the ends. Cracks are concentrated at the beam ends because the prestressing force is designed to counter the maximum self-weight moment in the beams, which occurs directly at mid-span. At the girder ends, without the moment to balance the prestressing force, tensile stresses at the top of the beam and compressive stresses in the strand's transfer length can cause cracking (WisDOT 2017).

Such beam end cracks are thought to have several possible sources. Hasenkamp et al. (2008) compiled, through a survey and literature review, multiple suggested sources of cracks in prestressed beam ends. Commonly cited causes of cracking are as follows:

1. Strand distribution: The amount and degree of cracking shows some relation to the number of draped strands in a beam. Although draped strands can be an effective way to raise the center of gravity of the prestressing force and reduce cracking (WisDOT 2017), using a large number of draped strands reportedly results in more cracking (Hasenkamp et al. 2008).

2. Detensioning method: A typical method of releasing the tension in prestressing strands is flame cutting. In this process, strands are individually cut using a torch. The result is a sudden release of tension and subsequent introduction of stresses into the concrete beam. In addition, these stresses are introduced unevenly, or asymmetrically, into the beam, which does not allow stresses to oppose and balance each other. Hydraulic detensioning allows for slower transfer of force and fewer cracks, but this method is less common and requires additional equipment (Hasenkamp et al. 2008).

3. Free strand length: Once strands at the end of one beam have been cut, the beam is compressed and experiences some shortening. This causes the lengths of any strands not embedded in the beam (i.e., the free strand length) to increase, creating tensile stress and strain. Free strands of shorter lengths experience greater strain and greater tensile force,

increasing the likelihood of cracks developing in the beam ends. Longer free strands can be utilized to reduce beam end cracking (Kannel et al. 1997).

4. Strand diameter: In order to achieve a higher prestressing force at the same stress level in strands, the use of 0.6 in. diameter as opposed to 0.5 in. diameter strands has increased relatively recently. A higher prestressing force also allows for the use of higher strength concrete. It has been observed that the use of 0.6 in. strands at the same spacing as 0.5 in. strands increases cracking in a beam (Hasenkamp et al. 2008).

Other sources of beam end cracking have been suggested in addition to those listed above. However, for the purposes of this report, exploring and understanding a few causes of beam end cracking is sufficient.

Infiltration of Corrosive Agents

Once cracks are introduced into a prestressed beam end, corrosive agents are able to penetrate the surrounding concrete and reach the embedded steel. For steel to undergo corrosion, the only agents required are oxygen and water. However, the corrosion of steel embedded in concrete requires the destruction of the passive layer created by the high pH of the concrete. This layer is destroyed either by reducing the concrete's alkalinity or increasing the concentration of chloride ions to a certain level. Iowa's bridges are among those particularly susceptible to high chloride concentrations due to the use of deicing salts and chemicals during the winter.

In an attempt to reduce the potential for moisture and chemical infiltration, cracks of a certain width are often sealed with a waterproofing agent at the precast plant. According to the respondents to a survey by Hasenkamp et al. (2008), epoxy injection is the most common method of sealing cracks. Some organizations take further precautions to mitigate moisture infiltration into beam ends. The Iowa DOT, for example, coats the end faces of all prestressed concrete beams with Sikagard 62, an epoxy coating (Hosteng et al. 2015). While such waterproofing measures are not in vain (although some substances prove more effective than others), it is thought that moisture may be present on the embedded steel before the beam end can be sealed. Hosteng et al. (2015) observed that several beams in a precast yard contained uncut strands extending beyond the beam end face, all of which were visibly rusted. Due to the gaps present between individual strands woven together to form prestressing strands, moisture may be able to migrate into the beam through capillary action. It is thought that this moisture present in beam ends prior to waterproofing may contribute to the initial rusting of the embedded steel, as well as the degradation of the waterproof seal itself (Hosteng et al. 2015).

Corrosion Process

Once moisture and chemicals (i.e., chlorides) have migrated through cracks, a beam end contains the necessary ingredients for corrosion to occur. First, as previously mentioned, a high enough concentration of chlorides destroys the passivating layer around the steel. At this point, corrosion is able to occur. Considering the length of one prestressing strand or reinforcing bar, the

corrosion process proceeds as follows. First, at one location, iron atoms donate electrons to the steel and the positive ferrous ions move to the concrete. Locations at which a material donates electrons to an electrochemical process are called anodes. The free electrons then move to a location in the steel with a lower energy level and react with water and oxygen that has penetrated the concrete. The product of this reaction is hydroxide ions. A location at which electrons are accepted as part of an electrochemical process is called a cathode. The positively charged ferrous ions then react with the negatively charged hydroxide ions to produce iron hydroxide, or rust. The reactions described above are shown as a series of chemical equations below:

$$2Fe \rightarrow 2Fe^{2+} + 4e^{-}$$

$$2H_2O + O_2 - 4e^{-} \rightarrow 4OH^{-}$$

$$2Fe^{+} + 4OH^{-} \rightarrow 2Fe(OH)_2$$

The formation of rust on embedded steel negatively affects a beam in two primary ways. First, because the iron in steel is a reactant in the corrosion process, some steel must be sacrificed to produce rust, reducing the effective cross-sectional area of the steel bars or strands. In the case of prestressing strands, designed to introduce large compressive forces into beams, this loss of material (and therefore area) may cause a reduction in the prestressing force being imparted on the beam. The result is a reduced capacity for the beam section. Second, corrosion also adversely affects a beam by creating internal tensile stresses. The product of corrosion reactions, rust, is less dense than the steel from which it was formed. That is to say, a certain mass of rust occupies a larger volume than an equal mass of steel. As a result, the formation of rust creates expansive tensile forces against the surrounding concrete. As corrosion continues, the low tensile strength of the concrete cannot resist the internal stresses, and spalling may occur. An obvious safety hazard, spalled beam ends result in reduced sections and possibly reduced bearing areas, if the spalling is near enough to the beam end.

Current Practices

In general, two approaches are used to address the deterioration of prestressed concrete beam ends: rehabilitation and retrofit. For the purposes of categorization, and to avoid potential confusion, this report defines each approach as follows. Rehabilitation is any technique involving the application of a component or mechanism designed to repair an already existing, damaged element of a prestressed concrete beam. A common example of a rehabilitation technique is patching of spalled concrete. Retrofit is any technique by which new, force-carrying elements are added to a prestressed concrete beam with the singular goal of increasing beam capacity. A retrofit repair method does not aim to restore an existing damaged component of a beam (e.g., spalled concrete) but rather is intended to add new elements that can carry load that the beam no longer can. A common example of a retrofit technique is the addition of near-surface mounted (NSM) rods in a beam soffit. It should be noted that in order to properly apply a retrofit repair technique, some degree of rehabilitation may be necessary. For example, if concrete has spalled at a location at which NSM rods are to be installed, the concrete would require patching before

the retrofit may take place. Current practices in rehabilitation and retrofit repairs are detailed in the following sections.

Rehabilitation

Patching

Patching of spalled concrete, although a relatively simple rehabilitation technique, is an important step in restoring a damaged beam. Applying a patch to a spalled concrete beam restores the section for which the beam was designed. In addition, spalling of a beam may likely expose embedded steel, which corrodes much more quickly when exposed to open air. While patching concrete is a relatively simple procedure, it requires care and attention to properly execute.

First, any unsound concrete must be removed from the damaged area to ensure a proper bond and the structural integrity of the beam section. To avoid creating feather edges in the patch, the edges should be saw cut at a shallow depth (Dominguez Mayans 2014). It is paramount not to cut too deep because prestressing strands may be damaged or severed (Dominguez Mayans 2014, Needham 2000). By the nature of the interaction between the patching material and the surrounding concrete, the bond between the materials is critical for the effectiveness of the patch. To increase the effective contact surface area, the surface of the damaged concrete should be roughened and dust or other fine particles should be removed from the contact area (Dominguez Mayans 2014). Any embedded steel that has been exposed as a result of spalled concrete should have the rust removed before patching. At this point, a suitable patching material may be applied. Suitable materials are those that meet the requirements for compressive strength, bond strength, thermal properties, etc. (Dominguez Mayans 2014).

A variety of materials can be used in concrete beam patch repairs. Mortar repairs are common for mild to moderately damaged beam ends. Patching with mortar succeeds in replacing lost concrete cover; however, this material fails to restore the original strength and stiffness of the girder (Shaw and Andrawes 2017). Normal concrete (NC) has also been used in repair methods (Figure 2.1) (Shield and Bergson 2018).

Shield and Bergson 2018, MnDOT

Figure 2.1. Reinforced shotcrete repair of a damaged beam end in Minnesota

However, as with mortar repairs, simply replacing the concrete cover lost to spalling is not sufficient. To restore the original capacity of the beam, further steps must be taken. A greater volume of concrete may be sufficient, but often the addition of reinforcing steel or other structural agents is required when using traditional patching materials. Some mortars specified by DOTs are specialized to resist chlorides. Other options include additional protective sealants to protect the beam from further water and chloride penetration in the future. Each step beyond the basic patching that is required for this type of damage adds more cost, effort, and traffic closure time (Chen and Duan 2014, Feldman et al. 1996, Hosteng et al. 2015).

Strand Splicing

In beams with severely damaged or severed prestressing strands, an available rehabilitation technique is strand splicing. As the name suggests, this repair method involves reconnecting the ends of a severed strand to form one continuous element. Typically, a turnbuckle connects the severed ends and introduces force back into the broken strand. Although the turnbuckle does experience loading as it tensions the strand, this report classifies strand splicing under rehabilitation because it is specifically meant to repair an existing, damaged element.

When circumstances have allowed it, strand splicing in situ has proven to be an efficient and cost-effective method of restoring tension in a damaged strand (Kasan et al. 2014). However, due to the geometry of prestressed beams, it may be difficult to repair a single strand without affecting others. In fact, the diameter of splices requires that they not be placed immediately adjacent to each other on neighboring strands but rather staggered by at least 2 in. (Kasan et al. 2014). In cases of very localized damage, this creates a potential issue. Additionally, the behavior of splices relative to the strands must be considered. For example, splices are much stiffer than the strands, resulting in different strain values for a given stress. This could lead to asymmetric behavior in a repaired section (Kasan et al. 2014). Though not without its limitations, strand splicing allows for the efficient repair of severely damages strands, particularly compared with superstructure replacement.

Electrochemical Corrosion Resistance

Unlike the previously discussed rehabilitation techniques, electrochemical corrosion resistance does not involve a structural repair meant to carry load. Instead, electrochemical corrosion resistance aims to mitigate the process of corrosion itself. Although somewhat time-consuming, electrochemical protection of embedded steel addresses the root of the problem with deteriorated beams. The ultimate goal of the repair technique is to introduce electricity to the steel so that it becomes negatively charged, forcing away negatively charges chloride ions.

As described above, electrochemical corrosion resistance works by supplying electrons to the embedded steel in order to force away negatively charged chloride ions (Clemena and Jackson 2000). Drawing chloride ions away from the steel allows the passivating layer between the steel and the concrete to begin reforming, slowing the corrosion process. In order to establish an electrochemical cell, the following components must be in place. First, an anode system is required to supply electrons to the steel (Clemena and Jackson 2000, ELTECH 1993). The anode material must be of a lower electronegativity than the steel (i.e., less inclined to attract electrons). With the anode system in place, a metallic connection must be made between the anode and the embedded steel at a minimum of one location (Clemena and Jackson 2000). The connection between the anode and cathode (in this case, the steel) allows for the flow of current between the two materials. Additionally, an electrolyte is required for the transfer of ions and electrons to and from the anode and cathode as current flows through the system (Clemena and Jackson 2000). Finally, an external source of current is required to supply electricity to the steel, forcing the electrochemical process and causing the corrosion process to run in reverse (Clemena and Jackson 2000, ELTECH 1993). In order to resist corrosion, the external source of current receives electrons from the anode system and supplies electrons to the cathode (Clemena and Jackson 2000). This results in a positively charged anode and negatively charged steel. Consequently, the negatively charged chloride ions near the steel are driven outward towards the anode system (Clemena and Jackson 2000).

The process discussed above is generally true for an electrochemical corrosion resistance technique. Two primary methods of applying this technique exist: electrochemical chloride extraction (ECE) and cathodic protection (CP). The two methods are very similar but have a small number of differences. First, ECE utilizes a liquid electrolyte that surrounds the anode system and allows electrons and ions to flow. This electrolyte must be maintained over the course of the treatment, approximately four to eight weeks (Clemena and Jackson 2000). Alternatively, CP uses conductive anode systems that do not require extensive maintenance, such as conductive coke-asphalt or conductive mastics (ELTECH 1993). Second, ECE requires that a larger area of concrete be covered by the anode and electrolyte compared to CP (Clemena and Jackson 2000). In other respects, the two methods are very similar. Both produce beneficial effects even after the system is removed. Specifically, the corrosion rate remains lower than that in untreated concrete for years after each system is removed from the beam (Clemena and Jackson 2000, ELTECH 1993). In addition, the costs of both methods are fairly similar (Clemena and Jackson 2000). The key differences between the two systems point to CP as the more convenient, preferred method.

Retrofit

Steel Jacketing

Steel jacketing of a beam has been used as a retrofit technique, but it is becoming less common as its popularity diminishes. The concept of the retrofit is to provide a kind of steel shell around a concrete beam, increasing the beam's capacity by offering additional flexural strength relative to a standard concrete beam (Harries et al. 2009). Though simple in theory, application of a steel jacket around a beam is significantly more difficult in practice. Jackets must often be welded together around a beam in the field, as opposed to prefabricated and slipped onto the beam. Additionally, studs or shear heads are required for shear transfer to prevent the jacket from simply sliding along the length of the beam once applied (Harries et al. 2009). These laborious tasks involved in the application of steel jackets still do not include the necessary protection from rusting when steel is exposed to the open air. All factors considered, steel jacketing is not a desirable long-term retrofit.

Bonded FRP Sheets

With the relatively recent advances in fiber-reinforced polymer (FRP) technology, bonded FRP sheets have become a competitive option for the retrofit of prestressed concrete beams. The principle of bonded FRP sheets as a retrofit is similar to that of steel jacketing; the additional strength of the sheets offers increased flexural capacity for the beam. Unlike steel jackets, however, the bond between the FRP sheets and the beam is achieved using an adhesive. This bond between the beam and the FRP sheets therefore serves as the mechanism of force transfer, making bond strength critical to the success of an FRP retrofit (Kalfat et al. 2013).

The most general application of FRP sheets as a retrofit technique is simply bonding an FRP laminate to a beam soffit. When the beam is loaded beyond the level at which the FRP is applied, the FRP sheet becomes engaged and carries some of the force in the tension face of the beam (Nguyen et al. 2013). Such retrofit techniques that do not carry any force until a certain level of loading is reached are referred to as passive retrofits. The typical failure mechanism of a beam retrofitted with FRP sheets is debonding of the sheets initiated by flexural cracks in the beam. As a result, it has been observed that when a small amount of FRP is used, increasing the length of the sheets increases the beam's stiffness but not its flexural strength (Nguyen et al. 2013). However, increasing the number of layers of FRP may increase the flexural capacity of the beam. Increasing the number of sheets up to three layers was found to increase the flexural strength of a beam while reducing the tensile strain in the embedded steel (Nguyen et al. 2013). Provided that an adequate bond surface is available, FRP sheets are a promising retrofit technique.

Although a viable retrofit option, FRP sheets are not used to their full structural capacity if failure is initiated by debonding. In order to address this issue, FRP stirrups (or U-wraps) have been applied to increase the bond between the sheets and the beam soffit (Figure 2.2).

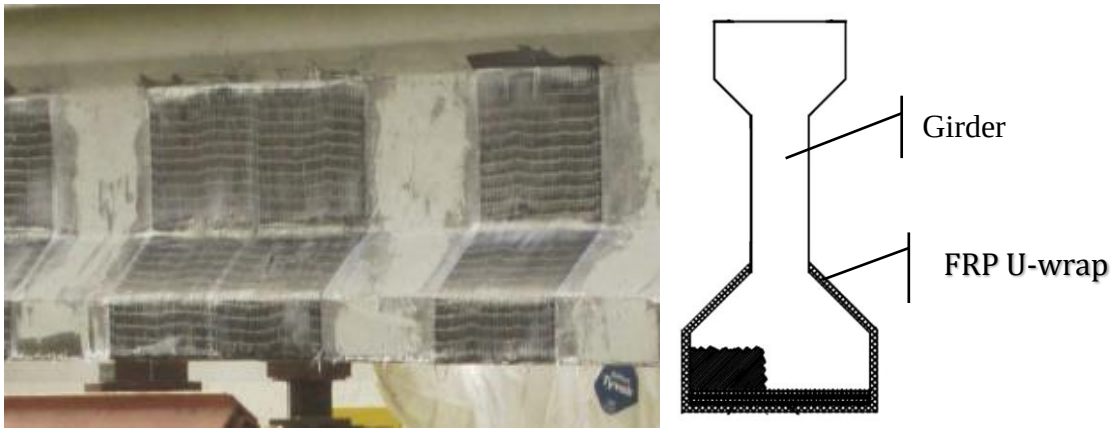

Figure 2.2. FRP stirrups (U-wrap) configuration

FRP stirrups, which mimic rebar stirrups, are applied transversely over longitudinal FRP sheets at a specified spacing. Stirrups are bonded to the beam by the same adhesive as the sheets; however, the bond occurs on the side of the flange or the web of the beam. As a result, stirrups provide an increased bond area over regions of the beam that are not as susceptible to cracking as the tension face (Kalfat et al. 2013). By reducing the likelihood of debonding failure, more of the FRP sheets' capacity may be utilized (Nguyen et al. 2013, Kalfat et al. 2013). However, the consequences of changing the failure mechanism from debonding to FRP rupture must be considered. Specifically, FRP behaves in a fairly brittle manner compared to the yielding of steel. Therefore, the joint failure mechanisms of brittle FRP rupture and ductile steel yielding must be accounted for in a beam retrofitted with FRP sheets and stirrups (Nguyen et al. 2013, Kalfat et al. 2013).

It should be noted that prestressing technology may also be applied to FRP laminate retrofits. During application, FRP sheets may be prestressed before bonding to the beam soffit. This action changes the retrofit from passive to active (Harries et al. 2009). That is to say, the prestressed sheets are always carrying force and contributing to the capacity of the beam. While prestressing FRP sheets has shown to result in a slight increase in flexural capacity, the process of prestressing the sheets is laborious and time-consuming. The benefit of fully prestressing FRP sheets does not appear to outweigh the costs of introducing prestress into the FRP (Harries et al. 2009). Additionally, the more brittle behavior of a beam with fully prestressed FRP sheets is undesirable. If a completely passive repair is not wanted, partially prestressing the FRP retrofit may be a desirable compromise (Harries et al. 2009).

NSM Rods

In terms of their effect on beam capacity, NSM rods behave very similarly to bonded FRP sheets. NSM rods are applied to the soffit of a beam where they may carry some of the tensile force in the bottom flange of a prestressed beam. The key difference between FRP sheets and NSM rods is that NSM rods are embedded just below the tension face of a beam while FRP sheets are bonded externally to the tension face (Harries et al. 2009). This places NSM rods within the concrete cover of the beam. A benefit of placing a retrofit just under the surface of the beam as

opposed to outside the beam is the high bond strength of the grout used to fill in the cavities made by the NSM rods. A strong bond helps to eliminate the potential for debonding failure that is observed with FRP sheets (Harries et al. 2009). Additionally, mounting rods within the concrete cover offers some protection from the elements that may not be available for an externally bonded retrofit.

Due to the protection of the concrete cover, NSM rods may come in the form of steel or FRP. However, as FRP becomes increasingly accessible, the issue of steel corrosion does not seem to make steel NSM rods worth the risk. NSM rods are also able to utilize prestressing technology to add extra capacity to a beam. Much like FRP sheets, however, prestressing NSM rods in situ is very labor-intensive and likely not worth the associated costs (Harries et al. 2009).

Externally Mounted Rods

Externally mounted rods behave just like NSM rods, but rather than residing in the concrete cover, externally mounted rods are fixed to the outside of the beam. Besides the different location, a key difference between external and NSM rods is the mechanism of force transfer. While force is transferred to NSM rods through the bond with the surrounding grout and concrete, force is transferred to external rods through some type of discrete anchor. A common example of an anchor for external rods is a bolster. Bolsters are either concrete or steel elements that are secured to the concrete beam and hold the external rods without slipping. As the beam experiences strain, the bolsters move with the beam and cause the external strand to carry some of the stress due to loading (Harries et al. 2009).

Although very similar to NSM rods, external rods exhibit a few key differences. First, external rods are much simpler to install than NSM rods. No large cavities must be made in the concrete cover; only bolt holes must be made at bolster locations. Alternatively, if concrete bolsters are used, bolt holes are not required. Concrete bolsters may be cast along with the beam or added later using a shear connection (Harries et al. 2009). While bolsters may be simple to install, it should be noted that they also result in much more localized force transfer. Under heavy loading, this may be undesirable. Additionally, external rods may be placed at different locations on the beam more easily than NSM rods. It is true that NSM rods may be placed anywhere from the beam soffit to the edges or top of the bottom flange; however, external rods may be applied almost anywhere that is appropriate. Freedom to place external rods almost anywhere on the beam may be desirable under certain conditions, but in general this characteristic provides the most benefit at the tension face of the beam where the corresponding moment arm is largest. Finally, a significant benefit of external rods compared to NSM rods is the ease of prestressing. By their very nature, bolsters act as anchors that the external rods may be jacked against. This action occurs while the rod and bolsters are in place, making it the ideal in situ prestressing technique (Harries et al. 2009).

It should be noted that external rods are clearly not protected from the elements like NSM rods are. However, because of the increasing popularity of FRP materials for retrofit applications, including external rods, the protection provided by concrete cover (i.e., corrosion protection) is

not a major concern. As a result, the ease of installation and prestressing provided by external rods may likely outweigh the benefit of the concrete cover that protects NSM rods.

Alternative Patching Materials

To achieve the best long-term results for the repair of concrete damaged by corrosion, materials with specialized properties are desired. For this study, two primary criteria were considered when choosing alternative patching materials. First, a sufficient bond strength is necessary to achieve a resulting structure that behaves monolithically. As noted above in the discussion on repair methods, an inadequate bond partially negates the desirable mechanical properties of the repair system. Second, to prevent continued damage from corrosive elements, low permeability and small crack widths are preferred to prevent the continued penetration of chloride-laden deck runoff. Prerequisite to these specialized properties, an adequate patching material must exhibit desirable mechanical properties such as strength, ductility, and durability.

The use of composite materials has demonstrated promise for concrete girder rehabilitation due to their desirable material behaviors and amenable application qualities. This section overviews various material options and the reasoning for the final material selections for this investigation.

Ultra-High Performance Concrete

For the structural restoration and retrofit of concrete bridges, ultra-high performance concrete (UHPC) has gained popularity in research and engineering practice. UHPC demonstrates much higher strength and much greater long-term durability than normal concrete. UHPC is composed of portland cement, pozzolans (primarily micro- and nano-silica), fine sand with optimized particle size distribution, steel fibers, normal water, superplasticizer, and other admixtures as required (Jafarinejad et al. 2019, Karim et al. 2019). The resulting composite demonstrates very high strength in compression, tension, and flexure. UHPC has low permeability, which allows for exceptional performance in harsh environmental conditions.

Although the implementation of UHPC has been limited due to the high production costs, the application of only small amounts for the repair of existing concrete structures has been successful in restoring and even enhancing the mechanical properties and durability of the original structure. The material's suitability for use in retrofits and its longevity make it a cost-effective repair strategy over the life of the structure. Many studies have also shown promising bond strength for UHPC, making it a good candidate for the repair of existing structures. With an adequate interface roughness, failure will occur in the plain concrete prior to failure at the material interface, indicating an effective bond between UHPC and plain concrete (Harris et al. 2015, Hussein et al. 2016). UHPC is a strong candidate for the repair of corrosion-damaged beam ends due to the material's high bond strength and its ability to restore capacity while preventing further corrosion without the need for additional sealants.

High Early Strength Concrete

A key factor in bridge repair is the speed of the repair time. For this reason, high early strength concrete (HESC) has been widely studied and implemented in roadway construction. There are many methods to create HESC, including the use of rapidly hydrating cements and chemical admixtures. Type III portland cement is specifically classified as providing high early strength, but other ASTM cement types can still be used to create HESC. Type III portland cement typically has smaller particle sizes compared to other cements. The smaller the particle size, the faster the cementitious material can achieve full hydration, which leads to higher heat of hydration and an increased rate of strength development. Portland cement is the most commonly utilized material for reaching high early strength; however, several proprietary cementitious products are also available. The key differences lie in the kilning process and the components added to accelerate strength gain. As mentioned, chemical admixtures can be used for early strength gain, such as in the patented 4x4 process developed by BASF Chemicals to produce concrete with a compressive strength of 4 ksi in four hours. These products are considerably more expensive than ordinary portland cements and therefore are typically used only in emergencies (Casanova et al. 2019, Ghafoori et al. 2017).

Recommendations

It is important to consider the current practices for prestressed concrete beam repair described above in light of the objectives and scope of this project. Specifically, the goal of the project is to restore the full capacity of beams experiencing deterioration and extend the service life of the bridge containing said beams. A particular focus is placed on retrofit concepts.

Considering the different elements within a prestressed concrete beam and the several repair methods designed to address them, it is clear that no single repair procedure applies effectively to all scenarios. Therefore, it is necessary to develop different guidelines for various levels of damage or deterioration. However, some repair techniques are a necessity when applicable. Patching of spalled concrete is required whenever a significant portion of concrete has been removed, especially if steel is exposed. Additionally, strand splicing is necessary when any prestressing strand is severed (or nearly severed) due to corrosion or impact. These techniques are necessities when applicable because without them the integrity of the beam and any subsequent repairs are compromised. In the following sections, more specific repair methods are discussed for three levels of damage: light damage, moderate damage, and severe damage. General criteria for damage categorization are outlined below; however, individual judgement is required to assess in-service beams.

Light Damage

A lightly damaged beam, for the purposes of this report, is a beam that shows early signs of corrosion (e.g., fine cracking, rust stains) but no spalling of the concrete. A beam showing light damage likely has not experienced a structurally significant reduction in capacity; however, the beam's capacity will be reduced if the damage continues. In such a beam, the corrosion process has already begun. Therefore, a preemptive retrofit will only be effective if it is applied before

the corrosion damage has become too severe. Consequently, it is necessary to address the issue of corrosion to prevent further damage.

For lightly damaged beams, it is recommended that cathodic protection be employed to reduce the rate of corrosion. As described above under Electrochemical Corrosion Resistance, CP halts corrosion during the time it is applied and slows the rate of corrosion drastically even after the CP system is removed (ELTECH 1993). Because beam capacity is effectively unchanged at this level of damage, a structural retrofit is not required or recommended. Instead, CP appears to be the most cost-effective solution because it prevents the corrosion damage from becoming more severe in the future (ELTECH 1993).

Further, CP is recommended over ECE primarily because a CP system does not require a liquid electrolyte. The performance of the two corrosion resistance techniques is very similar (Clemena and Jackson 2000). Therefore, the main distinction between the methods is the convenience that the CP system provides by not requiring the maintenance of a liquid electrolyte. Various anode materials have been tested for CP systems, including conductive mastics (ELTECH 1993). A conductive mastic anode system may be beneficial by providing waterproofing for the area over which the mastic is applied. The reasons discussed above make a CP system (with a conductive mastic anode) appear to be the best solution for a lightly damaged beam.

Moderate Damage

A moderately damaged beam is defined in this report as a beam showing signs of significant corrosion, small to medium sized cracks, and some delaminated or spalled concrete. As opposed to a lightly damaged beam, a moderately damaged beam has a reduced capacity relative to an undamaged beam. Corrosion has clearly occurred and progressed in a beam with moderate damage. Therefore, corrosion mitigation as well as a structural retrofit must be considered.

First, as stated above under Patching, any unsound concrete must be removed and patched before further repair takes place. After concrete patching, it is recommended that a CP system be applied to reduce the corrosion rate and extend the service life of the structure. Just like in the case of a lightly damaged beam, corrosion will continue if left untreated in a moderately damaged beam. Therefore, the useful life of the structural retrofit is dictated by the amount of corrosion damage in the beam. Application of a CP system prevents otherwise inevitable future damage from occurring.

In addition to a CP rehabilitation system, it is recommended that a moderately damaged beam receive a structural retrofit to restore lost capacity. Considering the definition of moderate damage used in this report, it is assumed that additional prestressing force from the retrofit is not required to restore beam capacity. Individual beam requirements are determined based on the judgement of the inspector and/or engineer. Assuming no additional prestressing force is necessary, the recommended retrofit for a moderately damaged beam is FRP sheets and stirrups bonded to the bottom and sides of the beam, respectively. This combination provides a reliable increase in beam capacity while utilizing all or most of the strength of the FRP retrofit (Kalfat et al. 2013). A drawback of this retrofit is the introduction of the joint failure mechanisms of the

FRP and steel. However, with proper design and placement of the FRP stirrups, a less brittle failure mode may be achieved (Kalfatet al. 2013). Finally, the relatively simple installation of FRP sheets and stirrups (provided they are not prestressed) makes them the most appealing retrofit technique for moderately damaged beams.

Severe Damage

A severely damaged beam, as defined in this report, is any beam exhibiting drastic corrosion of the embedded steel, large cracks, and significant spalling of the concrete. A severely damaged beam has a large reduction in capacity and may be a safety hazard if use of the structure continues.

Concrete patching is a clear necessity for any severely damaged beam. However, before the patching material is placed, a severely damaged beam must be checked for strands in need of splicing. Corrosion will have progressed relatively uninhibited in a beam with this level of damage. As a result, exposed strands may have rusted all or nearly all of the way through. Determination of which strands, if any, require splicing relies on the judgement of the inspector and/or engineer. Once the necessary strands have been spliced or it is determined that none require splicing, concrete patches may be applied.

Again, it is recommended that a CP system be installed to prevent further corrosion damage to the embedded steel. The reactants necessary for the corrosion of steel are already present in the concrete and embedded steel when patches are applied, and corrosion will continue after patching (Clemena and Jackson 2000). In order to mitigate the damage to the concrete and embedded steel, as well as damage to future retrofits, the corrosion process must be slowed down.

Along with a CP system, a severely damaged beam requires a structural retrofit to restore its significantly reduced capacity. Unlike a moderately damaged beam, it is assumed in this report that a severely damaged beam requires additional prestressing force supplied by the retrofit. Severe damage is assumed to reduce the capacity of a beam such that the beam cannot afford to endure a certain amount of load before the retrofit is engaged. Determinations regarding the capacities of individual beams, again, rely on the judgement of the inspector and/or engineer. Assuming additional prestressing force is required, the recommended retrofit for a severely damaged beam is prestressed externally mounted FRP rods. The primary benefit of this retrofit is the ease with which prestressing force may be applied to an in-service beam (Harries et al. 2009). Additionally, the placement of external rods may be tailored to meet the special requirements of the bridge. Finally, using FRP rods prevents the corrosion issues associated with exposed steel.

It should be noted that the bolsters that connect the external rods to a beam may limit the amount of prestress that can be applied. Because the areas of force transfer are constrained to each bolster, high levels of stress may develop in the bolsters if prestressing force limits are exceeded.

SMALL-SCALE BOND TESTING

This chapter summarizes the experimental program conducted to test patching materials for use in beam-end repairs. This study involved both small-scale and large-scale testing. Details on the materials, test specimen preparation, and laboratory test setup are described in this chapter. Testing took place in the Structural Engineering Research Laboratory at Iowa State University.

Introduction

Bond Strength Test Methods

The bond strength between concrete and various materials has been extensively researched. Past studies have shown that the measured bond strength is greatly dependent on which test method is used, making it difficult to obtain a clear and conclusive assessment of bond performance (Momayez et al. 2005). To determine bond strength under tensile stresses, three common test methods include the pull-off test, flexural beam test, and splitting cylinder tensile test. When evaluating bond performance under shear stresses, researchers typically utilize a direct shear or a slant shear strength test (Silfwerbrand 2003, Mindess et al. 2002).

The direct tension pull-off test follows ASTM C1583. This test is popular because the pull-off method can be performed both in situ and in a laboratory setting. By drilling a small partial shallow core in the concrete specimen, a direct tensile force is applied to a steel plate that has been bonded to the core's surface. This is considered an appropriate determination of tensile bond strength due to the single mode of stress. However, issues may arise when using this method. Pull-off tests are performed on relatively small samples compared to a total bond area, resulting in greater sensitivity to local effects, stress disturbances, and drilling-induced damage. This may lead to a large amount of scatter in the data measured from direct tension tests (Zanotti and Randl 2019). Additionally, the shear-controlled region of a beam is not likely to undergo pure tensile stresses at the patch interface. For this reason, a direct tensile test would not best represent field conditions for this application.

The flexural beam test for bonded materials is described in ASTM C78. Half of the beam is cast as the substrate and the other half is cast with the patching material. Placed under simply supported conditions and either single- or two-point loads, the interface is subjected to flexural tension. Again, with the focus of this project being predominantly on shear stresses, this method would not be ideal for this project.

The splitting tensile test uses concrete cylinders under indirect tension in accordance with ASTM C496. For evaluation of bond strength, half of the cylinder is cast as the substrate along the length of the cylinder and the patching material is cast on the other half. Specimens for this test are easily replicable. This method is further described in later sections of this report.

Bond strength under shear forces can be tested through direct shear to provide a clear demonstration of the slip behavior of bonded materials as well as to single out shear

performance. The steps required for direct shear testing are more complicated than for other types of tests. The preparation of the bond interface surface affects the test results as well as the bond area (Zanotti and Randl 2019, Liao et al. 2019, D'Antino et al. 2016).

Slant shear tests are performed by placing a compressive load on a specimen with the materials bonded on a slanted interface. Slant shear specimens can be rectangular prisms or cylindrical. The testing procedure follows ASTM C882. Typically, standard 4 in. by 8 in. or 6 in. by 12 in. cylinder molds are used in the manufacture of slant shear samples. The stress states experienced during this test method can occur in real-world structures. Factors affecting this test include interface surface preparation and the angle of the contact plane. Multiple studies have tested for the most appropriate bond angle to effectively determine bond strength (Zanotti and Randl 2019, Naderi 2009, Clark and Gill 1985).

Ultimately, two test methods were chosen to evaluate the bond performance of potential patching materials for this research project. Bond strength in terms of shear stress and tensile stress was determined using the slant shear strength test and the splitting tensile strength test, respectively. These methods were selected because they could easily be conducted within the facilities at Iowa State University, increasing repeatability among the multiple batches of patching material. Additionally, these tests attempt to replicate stress states that occur at the interface of a beam-end repair.

Effects of Interfacial Preparation

Concrete interfacial roughness plays a major role in the overall bond strength between old and new concrete. He et al. (2017) concluded that greater interfacial fractal dimensions contribute to higher new-to-old concrete mechanical strengths. Likewise, an interfacial adhesion agent was found to be beneficial to bonding. The study utilized iron combs of various sizes to generate artificial roughness (He et al. 2017). There are many other methods of modifying the interface layer for improving bond performance. Common methods applied in the field and for studies include but are not limited to wire brushing and sandblasting. Tools can be used to chip or groove the surface to increase the roughness level. Forming an interfacial surface from wet concrete is achieved in various ways. Applying a retarder to the forms allows for different levels of aggregate exposure. Combing a wet surface creates a roughened surface once the concrete has cured (Harris et al. 2015, Júlio et al. 2004, Carbonell Muñoz et al. 2014, Santos et al. 2007). In general, a roughness level similar to or greater than that produced by sandblasting is required for adequate bonding to successfully transfer forces between the old and new concrete.

Patching Materials

To achieve the best long-term results for the repair of concrete damaged by corrosion, materials with specialized properties are desired. For this study, two primary criteria were considered when choosing alternative patching materials. First, sufficient bond strength is necessary to achieve a resulting structure that behaves monolithically. As discussed above, inadequate bonds partially negate the desirable mechanical properties of the repair system. Second, to prevent continued damage from corrosive elements, low permeability and small crack widths are

preferred to reduce the continued penetration of chloride-laden deck runoff. Prerequisite to these specialized properties, patching materials must exhibit adequate mechanical properties such as strength, ductility, and durability.

Conventional Concrete and Cement Mortar

A common material used in concrete girder bridge repair is normal concrete or cement mortar. Often utilized for mildly to moderately damaged beam ends, patching with NC or mortar succeeds in replacing lost concrete cover; however, this material fails to restore the original strength and stiffness of the girder (Shaw and Andrawes 2017). In some cases, it is sufficient to install a greater volume of concrete in order to restore capacity, but often the addition of reinforcing steel or other structural agents is required (Shield and Bergson 2018). A number of DOT-specified mortars are specialized to resist further chloride infiltration. Other options include the application of protective sealants to inhibit water and chloride penetration. Each of these additional steps and requirements increases the cost, effort, and traffic closure time for repairs (Iowa DOT 2014, Feldman et al. 1996, Hosteng et al. 2015).

Ultra-High Performance Concrete – Proprietary

For the structural restoration and retrofit of concrete bridges, UHPC has gained popularity in research and engineering practice. UHPC denotes cement-based materials demonstrating much higher strength and ductility and much greater long-term durability than normal concrete (Shi 2015). UHPC is typically composed of portland cement, pozzolans (primarily micro- and nano-silica), fine sand with optimized particle size distribution, steel fibers, normal water, superplasticizer, and other admixtures as required (Jafarinejad et al. 2019, Karim et al. 2019). The resulting composite demonstrates very high strength in compression, tension, and flexure. UHPC has low permeability, which allows for exceptional performance in harsh environmental conditions.

Although the implementation of UHPC has been limited due to the high production costs, the application of only small amounts for the repair of existing concrete structures has been successful in restoring and even enhancing the mechanical properties and durability of the original structure. The material's suitability for use in retrofits and its longevity make it a cost-effective repair strategy over the life of the structure. Many studies have also shown promising bond strength for UHPC, making it a good candidate for the repair of existing structures. With an adequate interface roughness, failure will occur in the plain concrete prior to failure at the material interface, indicating an effective bond between UHPC and plain concrete (Harris et al. 2015, Hussein et al. 2016). UHPC is a strong candidate for the repair of corrosion-damaged beam ends due to the material's high bond strength and its ability to restore capacity while preventing further corrosion without the need for additional sealants.

Ultra-High Performance Concrete – Nonproprietary

As previously stated, UHPC demonstrates promising qualities as a repair and rehabilitation material. However, a common factor limiting the use of UHPC is its high cost compared to conventional materials. Researchers at Iowa State University have been developing a nonproprietary alternative to the proprietary options for UHPC currently on the market. This nonproprietary UHPC mixture has demonstrated characteristics similar to those of proprietary designs (Karim et al. 2019). To diversify patching possibilities, this small-scale study included this nonproprietary UHPC (UHPC-NP).

High Early Strength Concrete

A key factor in bridge repair is the speed of the repair time. For this reason, HESC has been widely studied and implemented in roadway construction. There are many methods to create HESC, including the use of rapidly hydrating cements and chemical admixtures. Type III portland cement is specifically classified as providing high early strength, but other ASTM cement types can still be used to create HESC. Type III portland cement typically has smaller particle sizes compared to other cements. The smaller the particle size, the faster the cementitious material can achieve full hydration, which leads to higher heat of hydration and an increased rate of strength development. Portland cement is the most commonly utilized material for reaching high early strength; however, several proprietary cementitious products are also available. The key differences lie in the kilning process and the components added to accelerate strength gain. As mentioned, chemical admixtures can be used for early strength gain, such as in the patented 4x4 process developed by BASF Chemicals to produce concrete with a compressive strength of 4 ksi in four hours. These products are considerably more expensive than ordinary portland cements and therefore are typically used only in emergencies (Casanova et al. 2019, Ghafoori et al. 2017).

Shrinkage Compensating Cement Concrete

Early-age cracking (up to 24 hours after casting) may become problematic in concrete. It can have a negative effect on the aesthetics of the structure and decrease the structure's durability and serviceability by facilitating the ingress of harmful materials into the concrete bulk. Moreover, these cracks may expand gradually during the member's service life due to long-term shrinkage and/or loading. Early-age cracking is caused by two driving forces: (1) plastic shrinkage cracking, which is a physical phenomenon and occurs due to rapid and excessive loss of moisture, mainly from evaporation, and (2) chemical reactions between cement and water, which causes autogenous shrinkage. One method to limit the effects of early-age cracking is the use of shrinkage compensating cement concrete (SCC-C). Expansive components are added to cement to counter the shrinkage that occurs with portland cement. The development of this concrete type started in the 1950s when a chemical compound (C_4A_3S), known as Klein's compound, was mixed with portland cement (Bescher 2018, Russell et al. 2002, Mather 1970, Chen et al. 2012, Shi 2015). ASTM C845 specifications detail the tests and qualifications for this Type K cement. Use of this material for the repair of damaged beam ends would be beneficial

because the material would not easily be penetrated by harsh agents from the environment, which would mitigate further corrosion of the section.

Experimental Program

This section summarizes the experimental program conducted for testing the bond performance of patching materials to be used in beam-end repairs. This study involved multiple types of small-scale testing. Bond strength in shear and tension specimens was determined using the slant shear strength test and the splitting tensile strength test, respectively. Details on the materials, test specimen preparation, and laboratory test setup are described in this section. Specimen preparation took place in the Portland Cement Concrete Laboratory and testing took place in the Structural Engineering Research Laboratory at Iowa State University.

Materials and Properties

Conventional Concrete

The mix used to represent conventional or normal concrete in the small-scale portion of this research project was the Iowa standard C-4WR mixture. NC was used as the substrate material for all bonding tests performed. This concrete is specified to have a 28-day compressive strength of 4,000 psi, minimum. Mix proportions are listed in Table 3.1.

Table 3.1. Conventional concrete mix design

Components	lb/yd^3
Cement Type I	474
Fly ash - Class C	119
Coarse aggregate	1,517
Fine aggregate	1,500
Water	255
HRWR	3

Ultra-High Performance Concrete – Nonproprietary

The materials used for the nonproprietary UHPC (UHPC-NP) mixture for this study consisted of cement, silica fume, fine aggregate, masonry sand, steel fiber, high-range water reducing (HRWR) admixture, and water. The cement was ASTM Type I cement with a specific gravity of 3.10. The fine aggregate was clean river sand (i.e., between 0.00 and 0.1870 in. in diameter). The fine aggregate was sieved to limit the maximum size to 0.0937 in. The specific gravity of the fine aggregate was 2.72. The masonry sand was obtained from a local supplier in Ames, Iowa. To obtain the desired particle packing in the mix, the masonry sand was included to form 15% of the total sand, following the Andreasen-Andersen particle packing curve. The steel fibers had a

diameter of 0.0079 in. and a length of 0.5120 in. The basic material properties and the mix proportions for UHPC-NP are listed in Table 3.2 and Table 3.3, respectively.

Table 3.2. Basic characteristic properties of UHPC-NP

Property	Typical value
Flow (in)	8.5
Split tensile strength (ksi)	1.5
7-day compressive strength (ksi)	14.2
Resistivity (kΩ-in)	3.3
Ultimate autogenous shrinkage (με)	240
Ultimate drying shrinkage (%)	0.135

Table 3.3. UHPC-NP mix design

Components	lb/yd^3
Cement	1,637
Silica fume	115
Masonry sand	898
Regular sand*	739
Water	350
Steel fibers$^+$	234
HRWR	77

*Sand passing 600 microns sieve, $^+$2% by volume

Ultra-High Performance Concrete – Proprietary

The proprietary UHPC (UHPC-P) mixture utilized in this study was developed by LafargeHolcim and has a commercial name of Ductal. The basic properties of UHPC-P are presented in Table 3.4.

Table 3.4. Basic characteristic properties of UHPC-P

Property	Typical value
Total shrinkage at 90 days (με)	500
Tensile strength at 28 days (ksi)	1.3
Compressive strength on cube at 28 days (ksi)	18
Water porosity at 90 days (%)	6
Diffusion coefficient of chloride ions at 90 days (ft^2/s)	$\leq 1.1 \times 10^{-12}$
Apparent gas permeability at 90 days (ft^2)	$\leq 5.3 \times 10^{-18}$

The materials for UHPC-P consisted of a premix binder that comprised all cement, fine sand, silica fume, and silica powder, along with other proprietary materials that were not disclosed by the manufacturer. Based on the observed properties, the powder-like premix binder of this

mixture also contained a type of shrinkage reducing or shrinkage compensating ingredient. The other materials used in UHPC-P were a polycarboxylate-based high-range water reducing superplasticizer admixture, water, and steel fiber. The steel fibers in this mix were the same as those used in the UHPC-P mix. The mix proportions for UHPC-P are listed in Table 3.5.

Table 3.5. UHPC-P mix design

Components	lb/yd^3
Premix	3,700
Water	219
Super plasticizer	51
Steel fiber	263

High Early Strength Concrete

The research team conducted preliminary testing to determine the mix design variables required for HESC to be used as a functional patching material. The accelerator dosage was determined by creating trial batches for the control mix until the minimum 12-hour compressive strength of 3,000 psi was obtained. Additionally, the confined layout of the formwork in the large-scale portion of this project required the mix to have excellent workability so that it could be poured and completely fill the patch area. To achieve this, the mix was made to be a self-consolidating concrete (SCC). Water reducer was added to achieve SCC conditions in accordance with ASTM C1611. The mix design used in this project had a slump flow of 23 in., exceeding the 20 in. requirement to qualify as self-consolidating (Figure 3.1).

Figure 3.1. Slump flow of self-consolidating concrete mixture

Note that the platform for the slump flow test is imprinted with a 20 in. diameter ring surrounding the center where the slump form is placed. The sample in the figure is completely

covering that dimensioned ring and therefore surpasses its limits. The materials used for the HESC mix consisted of cement, fly ash, coarse and fine aggregate, an accelerating admixture, a polycarboxylate-based high-range water reducing superplasticizer admixture, and water. The cementitious components included 80% Type III portland cement with 20% Class C fly ash as a cement substitute for greater workability and long-term durability. The coarse aggregate consisted of 3/8 in. maximum size crushed limestone. The fine aggregate was clean river sand. The smaller size of the coarse aggregate was selected over the more typical 1 in. maximum size aggregate to limit any blockage that may occur in the narrow formwork of the beam patch. The water-to-cementitious materials ratio was 0.3 to ensure high strength. The 28-day compressive strength of this mix was 13,000 psi. The mix proportions for the HESC tested in this study are listed in Table 3.6.

Table 3.6. HESC mix design

Components	lb/yd^3
Cement Type III	640
Fly ash - Class C	160
Coarse aggregate	1,591
Fine aggregate	1,543
Water	279.5
Accelerator	12.9
HRWR	14.4

Shrinkage Compensating Cement Concrete

The materials used for the SCC-C mix consisted of two types of portland cement, fly ash, coarse and fine aggregate, a high-range water reducing superplasticizer admixture, and water. The cementitious components included 68% Type I portland cement, 12% Type K portland cement, and 20% Class F fly ash as a cement substitute for greater workability and long-term durability. The coarse aggregate consisted of 1 in. maximum size crushed limestone. The fine aggregate was clean river sand. The water-to-cementitious materials ratio was 0.4. The 28-day compressive strength of this mix was 8,950 psi. The mix proportions for the SCC-C tested in this study are listed in Table 3.7.

Table 3.7. SCC-C mix design

Components	lb/yd^3
Cement Type I	403
Cement Type K	71
Fly ash - Class F	119
Coarse aggregate	1,517
Fine aggregate	1,500
Water	255
HRWR	3.0

Interface Treatment

To compare the effects of the surface roughness of the interface between conventional concrete and the patching materials, three levels of roughness were studied for this research. Unroughened (UR) samples had a relatively smooth interface surface because they were cast against foam forms. Roughened samples were achieved by applying a chemical retarder to the mold before pouring the concrete (Figure 3.2).

Figure 3.2. Formwork retarder application

After 24 hours, each roughened specimen was washed to remove the unset material and expose the aggregate. Mid-roughened (MR) samples had a theoretical peak-to-valley depth of 3/8 in. Large-roughed (LR) samples had a theoretical peak-to-valley depth of 5/8 in. Sample specimens showing each surface type are presented in Figure 3.3.

Unroughened Mid-roughened Large-roughened
(a)

Unroughened Mid-roughened Large-roughened
(b)

Figure 3.3. Various levels of surface roughness for the substrate specimens: (a) slant shear specimens and (b) splitting tensile specimens

Splitting Tensile Strength Test

Overview

Splitting tensile strength testing was used to evaluate the bond performance under tensile stresses. During this test, the interface is put in a state of indirect tension by applying a compressive load along the longitudinal length of the cylinder, in-plane with the interface (Figure 3.4).

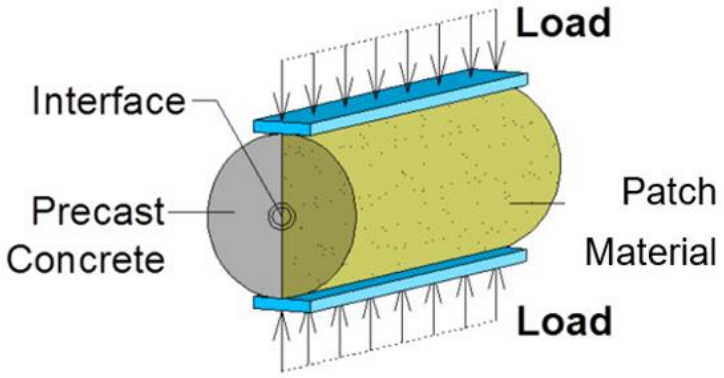

Figure 3.4. Splitting tensile strength test for characterizing bond strength

The research team performed this test in accordance with ASTM C496. Assuming failure at the interface of the two materials, bond strength can be estimated from the measured ultimate compressive force using Equation 1.

$$\boldsymbol{T = \frac{2P}{\pi l d}} \quad (1)$$

where *T* is the tensile stress (adhesion) in the interface, *P* is the ultimate compressive force applied during the test, *l* is the length of the concrete cylinder, and *d* is the diameter of the concrete cylinder.

Specimen Preparation

For this test, cylindrical specimens with a 4 in. diameter and an 8 in. height are formed from two materials connected by an interface along their length through the center of the cylinder (Figure 3.5). A foam insert is placed inside to create a half-specimen.

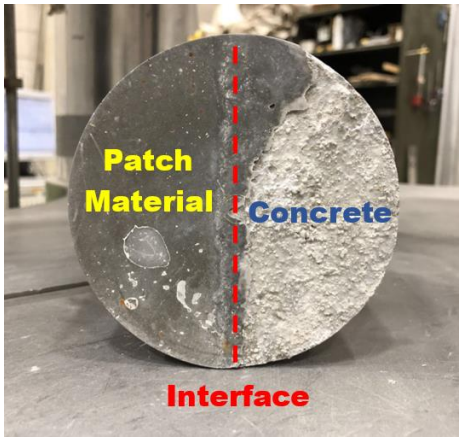

Figure 3.5. Splitting tensile test sample specimen

In this research, the conventional concrete half was cast and then cured for 28 days, after which the substrate was placed in the mold again and the second half of the specimen was cast using the patching materials. Both the NC and patching materials were poured in three layers. Each layer was compacted to ensure that the mold was filled uniformly and the final surface was level.

Slant Shear Strength Test

Overview

Slant shear testing was used to evaluate the bond strength under simultaneous compression and shear stresses. This test was performed in accordance with ASTM C882. The shear and normal compressive stresses at the material interface can be estimated from the measured ultimate compressive force using Equations 2 through 4.

$$\sigma_c = P/A_c \tag{2}$$

$$\sigma_n = \sigma_c \sin^2(\alpha) \tag{3}$$

$$\tau = 0.5\sigma_c sin(2\alpha) \tag{4}$$

where σ_c is the axial compressive stress at failure, σ_n is the normal compressive stress in the shear surface, P is the ultimate compressive force applied during the test, α is the angle of the shear surface from vertical, A_c is the area of the loading surface (circle), and τ is the shear stress in the shear surface (Figure 3.6).

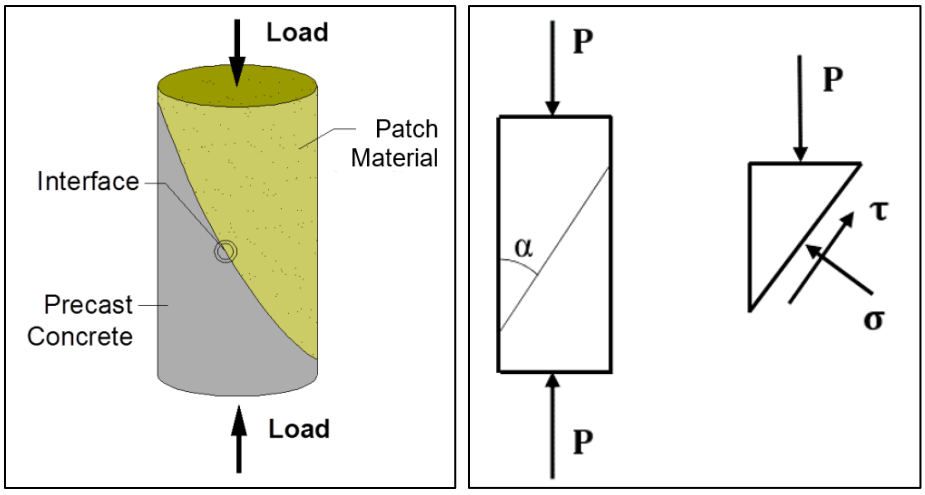

Figure 3.6. Slant shear test for characterizing bond (left); slant shear stresses (right)

Specimen Preparation

For this test, cylindrical specimens with a 4 in. diameter and an 8 in. height are formed from two materials connected by a diagonal interface that is 30° from vertical. A foam insert is placed inside to create the inclined surface (Figure 3.7).

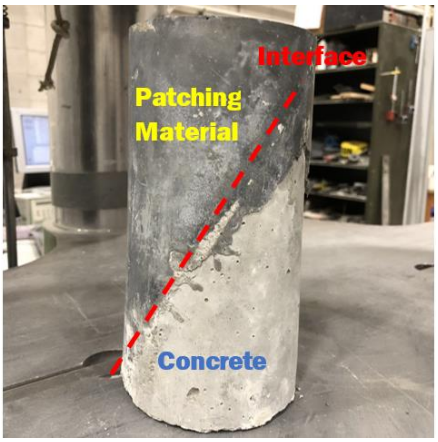

Figure 3.7. Slant shear test sample specimen

The same curing process used for the splitting tensile specimens was performed for these specimens. Again, both the NC and patching materials were poured into the mold in three layers. Each layer was compacted by vibration to ensure that the mold was filled uniformly.

Results and Discussion

Splitting Tensile Strength Test

All material types demonstrated excellent bond strength in tension, and the bond strengths did not appear to be affected by the roughness level of the interface. The adhesion stress at the time of failure was calculated for each sample. The true adhesion strengths could not be determined because at least some partial substrate failure was observed in all specimens. However, compared to the stress at failure observed in the plain (unbonded) material, the bonds between the patching materials and the substrates proved effective. As expected, both types of UHPC exhibited excellent tensile strength compared to the plain (unbonded) material. Figure 3.8 illustrates that the theoretical adhesion stress at failure for the two high-strength concrete types (HESC and SCC-C) exceeds that of the plain (unbonded) material.

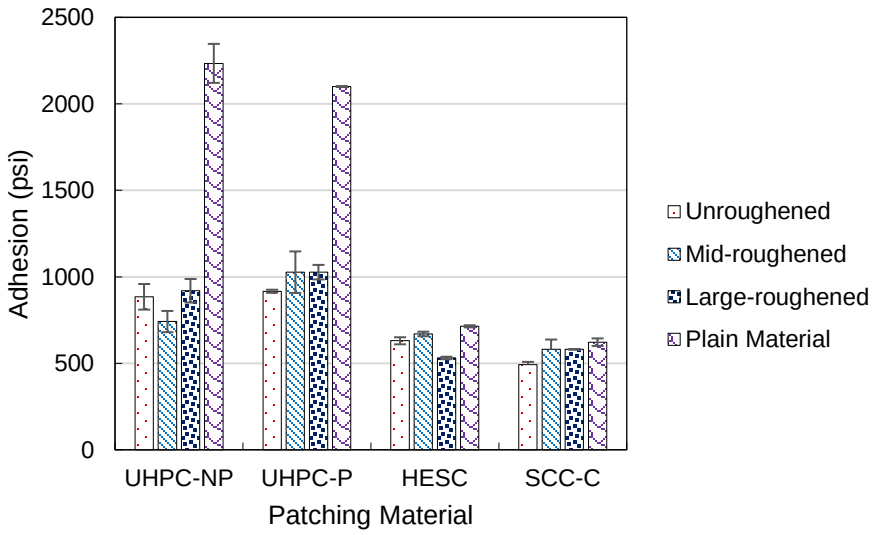

Figure 3.8. Adhesion stress at failure for different patching materials

Figure 3.9 shows a broken UHPC-NP specimen after failure, with fragments on the right showing the substrate and the portion of substrate material that had remained bonded to the UHPC-NP. The condition of this sample indicates that failure of the substrate likely occurred before the higher strength UHPC-NP failed, resulting in much higher peak loads recorded by the testing machine.

Figure 3.9. Example of UHPC-NP specimen after failure

Figure 3.10 shows examples of partial substrate failures for the HESC and SCC-C specimens.

Figure 3.10. Examples of partial substrate failure: HESC (left), SCC-C (right)

The adhesion values are summarized in Table 3.8.

Table 3.8. Theoretical adhesion stress at failure

Material	Roughness	Adhesion (psi)
UHPC-NP	Large-roughened	919
	Mid-roughened	741
	Unroughened	884
	Plain material	2,234
UHPC-P	Large-roughened	1,088
	Mid-roughened	1,027
	Unroughened	916
	Plain material	2,100
HESC	Large-roughened	531
	Mid-roughened	669
	Unroughened	630
	Plain material	714
SCC-C	Large-roughened	628
	Mid-roughened	580
	Unroughened	493
	Plain material	622

Slant Shear Strength Test

All slant shear specimens failed in compression, with none failing at the bond interface. The compressive failures for the HESC and SCC-C specimens always initiated in the substrate. These substrate cracks propagated through the full cylinder most commonly in form of nearly vertical splitting cracks before the interfacial shear stresses reached the maximum bond strength (Figure 3.11).

Figure 3.11. Examples of failed slant shear specimens: HESC (left) and SCC-C (right)

In contrast, in both types of UHPC samples, failure was localized in the substrate. Some cracking was visible into the UHPC material, but these cracks were arrested by the steel fibers in the UHPC mixes (Figure 3.12).

Figure 3.12. Examples of failed UHPC slant shear specimens

Table 3.9 summarizes the calculated interfacial shear stresses at failure. Due to the failure of the substrate concrete prior to failure at the bond surface, the true bond strengths under shear stresses did not reach their maximum values.

Table 3.9. Interfacial shear stress at failure

Material	Roughness	σ_c (psi)	τ (psi)	Failure mode*
UHPC-NP	Large-roughened	5,701	2,469	NC
	Mid-roughened	3,764	1,630	NC
	Unroughened	4,096	1,774	NC
UHPC-P	Large-roughened	8,935	3,869	NC
	Mid-roughened	7,517	3,255	NC
	Unroughened	6,216	2,692	NC
HESC	Large-roughened	5,466	2,367	NC
	Mid-roughened	3,832	1,659	NC
	Unroughened	4,296	1,860	NC
SCC-C	Large-roughened	4,211	1,824	NC
	Mid-roughened	4,047	1,753	NC
	Unroughened	4,061	1,758	NC

*NC – Failure initiated in normal concrete

Summary and Conclusions

Small-scale bond testing for this project consisted of testing four different materials to determine their bonding properties and their suitability for use as patch repair materials. The materials tested included proprietary and nonproprietary UHPC, HESC, and SCC-C. Each material was tested under tensile stresses and shear stresses using the splitting tensile strength test and the slant shear strength test, respectively.

All material types demonstrated good tensile bond strength. The interface surface condition did not demonstrate a significant effect on tensile bond strength for all samples. Both the HESC and SCC-C bonded samples exhibited a tensile bond strength exceeding the tensile strength of the plain (unbonded) samples tested. Both types of UHPC samples resulted in higher peak loads resisted. However, for all specimens, the substrate concrete failed before the testing machine reached peak load. Therefore, maximum tensile bond stress could not be determined.

All material types demonstrated good shear bond strength. No bond failures were observed during slant shear testing. In the case of the HESC and SCC-C samples, failure initiated in the substrate concrete and cracking propagated as vertical splitting cracks in nearly all specimens. Pure substrate failure occurred for the UHPC samples. Some cracks penetrated the UHPC but were mitigated by the steel fibers in the mix. These results suggest that all materials provide adequate bond strength and are suitable for use as patch repair materials.

FULL-SCALE BEAM PATCHING TESTING

This chapter summarizes the full-scale experimental program conducted on six segments of a prestressed concrete bridge girder. Details on the test specimens and the laboratory test setup are covered in this chapter.

Specimen Preparation

The beam used for testing was an Iowa DOT bulb-tee C-shaped beam measuring 115 ft in length (BTC115 beam) (Figure 4.1).

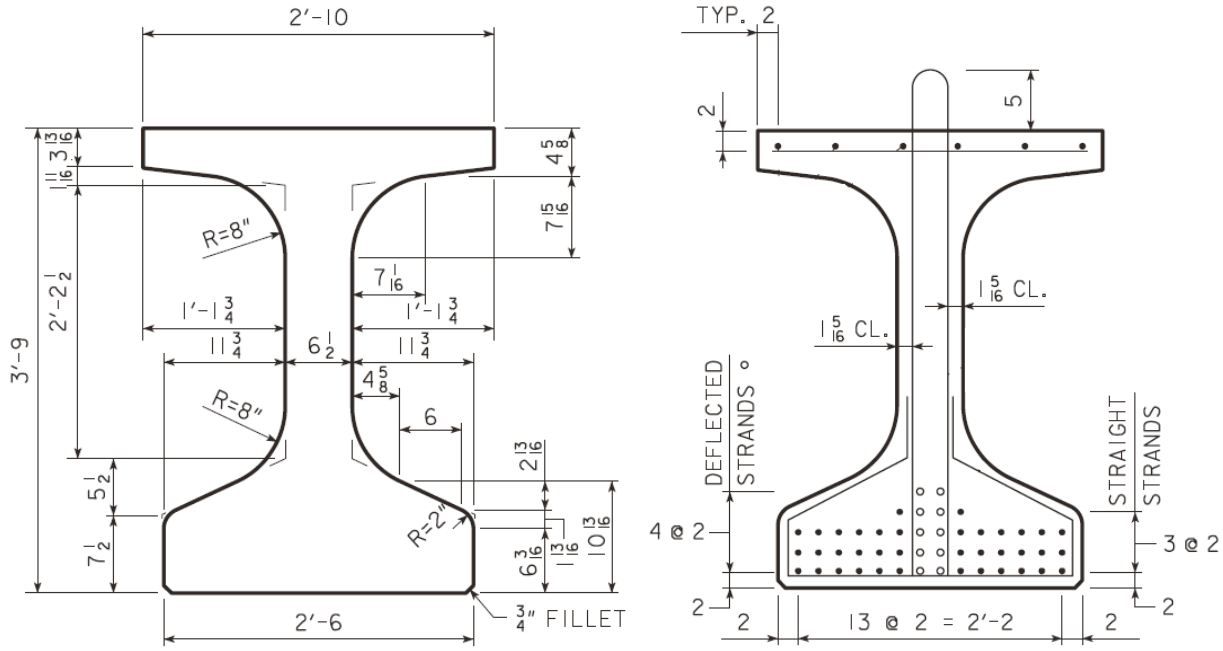

Figure 4.1. BTC115 cross-section (left) and midspan reinforcement layout (right)

This beam was provided for this research project by Forterra Building Products located in Iowa Falls, Iowa. The steel used for the prestressing strands had, at some point, been processed outside of the United States, which does not comply with requirements for use on government projects. However, it is important to note that the beam had not been rejected for unacceptable cracking during prestressing or any other structural property.

Cutting the Beam Segments

To cut the BTC115 beam, a wire saw method was chosen. The cutting mechanism for this type of saw involves a spinning diamond-studded wire being pulled through the concrete beam (Figure 4.2).

Figure 4.2. Wire saw cutting in progress

It was more desirable to use a wire saw than a hand-held circular saw because the wire saw reduces cutting time and labor costs while resulting in a cleaner edge. Two end pieces 2 ft 5 in. in length were cut from the BTC115 beam and discarded as scrap to avoid the large amount of shear reinforcement in that zone. The remaining beam was then cut symmetrically in order to reduce variation due to changes in tendon profile. The result was eight mirrored beam segments that could be used in direct comparison to each other. Each segment was cut to 11 ft to ensure the beams would fail in shear as opposed to bending (Figure 4.3).

Figure 4.3. Cut beam segment marked for artificial damage

Simulated Damage to Beam Ends

To investigate the effect of deterioration at the beam ends of bridge girders, the beams were artificially damaged to simulate damage caused by corrosion. Since the focus of this study is on the shear capacity of the girders, damage was focused on the webs of the beams. Additionally, half of the specimens were artificially damaged on the bottom flange at the beam ends. Figure 4.4 shows the artificially damaged areas of the beam specimens.

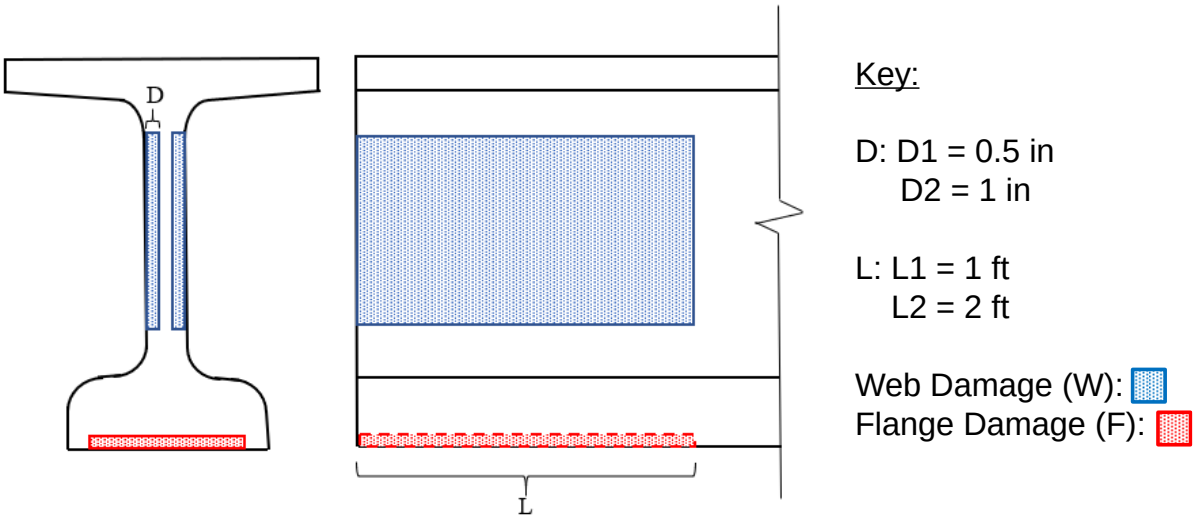

Figure 4.4. Areas of simulated damage on beam specimens

The region of concrete removed from the beam web resulted in an approximately 30% reduction of the width and cross-sectional area of the beam web. Each beam web had a damaged region with a height of approximately 1 ft, while the length of the area varied between 1 ft and 2 ft, as shown in Figure 4.5. The concrete was removed from the beam web by first cutting a grid with a depth of 1 in. Next, a hammer drill with a chisel attachment was used to remove the concrete within the grid, with care taken not to damage the stirrups. This process was repeated on both sides of the web and on each end of the specimen, and a similar process was used to remove concrete from the bottom flanges (Figure 4.5).

Figure 4.5. Cutting and chiseling (left), damaged bottom flange (center), and damaged web (right)

The ends of each beam are referred to as east and west, and the sides are referred to as north and south.

An example of a final damaged specimen is shown in Figure 4.6.

Figure 4.6. Artificially damaged beam specimen (1 ft damage)

The use of simulated damage allowed for consistent reproduction of the damaged areas on each specimen so that the specimens could be tested and compared. Table 4.1 shows the dimensions and location of damage on each beam specimen.

Table 4.1. Dimensions and location of damage on each beam specimen

Beam section	Damage length, ft	Damage to bottom flange
L1	2	Yes
L2	2	No
L3	1	Yes
L4	1	No
R4	1	No
R3	1	Yes
R2	2	No
R1	2	Yes

Overview of the Patching Plan

Six of the eight beam specimens cut from the BTC 115 beam were tested in the full-scale portion of this research project. The beams are labeled L1 through L4, R2, and R3. Two beams were left unpatched/unrepaired, two beams were patched with HESC, and two beams were patched with UHPC (NP). Details about the beams, including the names used in reporting results, are displayed in Table 4.2.

Table 4.2. Damage and patching details of beam segments

Name	Beam section	Damage length, ft	Bottom flange damage	Patching material
HESC-1	L1	2	Yes	HESC
Control-1	L2	2	No	--
Control-2	L3	1	Yes	--
HESC-2	L4	1	No	HESC
UHPC-1	R2	2	No	UHPC
UHPC-2	R3	1	Yes	UHPC

As stated in the previous section, the BTC115 beam was cut to have mirrored beam sections. The mirrored pairs for direct comparison are Control-1 and UHPC-1, and Control-2 and UHPC-2. The HESC specimens had different damage and shear reinforcement layouts.

Patch Fabrication Procedure

The four beams to be repaired were prepared for patching by first cleaning with a wire brush to remove large debris and power washing to remove any remaining dust and debris. Formwork was applied around each patch area so that the patch mix could be poured into the form at one end and the pressure head created would fill the damaged region completely. It should be noted that this exact forming method would not be used in the field due to limited access to the beam end area. Prior to pouring the patch mix, the concrete area to be patched and the formwork was wetted to limit water loss from the mix (Figure 4.7).

Figure 4.7. Beam patching formwork (left) and wetted area to be patched (right)

Workers transported the patch mix using buckets and poured the mixture into the forms until full. As the damaged areas filled with patching, more mix was added to fill the forms completely (Figure 4.8).

Figure 4.8. Patch mix being poured into formwork

Weep holes in the formwork were plugged when the mixture began draining (Figure 4.9).

Figure 4.9. Patch mix flowing from weep holes

Damaged regions on the bottom flanges were filled with patch mix and required no formwork. Test cylinders were cast from each patch mix to test compression strength over time. Identical methods of forming and patching were used on both the UHPC specimens and the HESC specimens.

Test Setup and Procedure

Loading Setup

Testing was performed to ensure that the maximum shear stresses occurred in the beam ends and that shear would be the resulting failure mode. To test the shear reaction of the beams in this study, four-point bending tests were carried out on the beam segments. The test setup is shown in Figure 4.10.

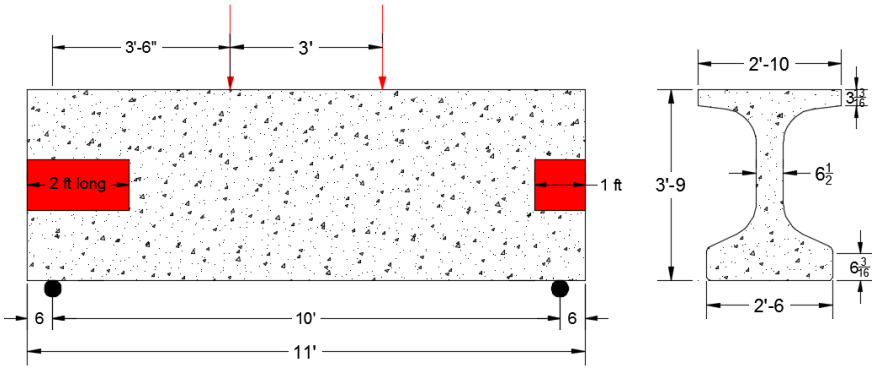

Figure 4.10. Four-point loading laboratory test set up

The beam segments were simply supported with a hinge and a roller. The center-to-center span between supports was 10 ft. This configuration creates a low span-to-depth ratio, inducing the development of shear cracks. Two 10 in. by 10 in. steel plates were placed on the top surface of the beam to distribute the load to the beam. The two point loads were located 3 ft apart, symmetrical by the center of the beam span. Each point load was applied using two hydraulic actuators and measured using 200 kip load cells.

Loading Protocols

During the first beam test, initial loading was applied in 25 kip increments until the capacity of the actuators was reached. Cracking on the beam surface was tracked at 100 kip increments. After initial loading, the beam was loaded to the maximum and unloaded for three additional cycles. Cracking and crack propagation were tracked at each additional maximum loading. After completion of the first beam test, a load increment of 50 kips rather than 25 kips was used for the initial loading on the remaining beams.

Instrumentation and Data Recorded

Three types of instruments were used for this study: string potentiometers, concrete strain gauges, and DC linear variable differential transformers (LVDTs).

The string potentiometers were located at the quarter points of the span (i.e., 2.5 ft from the supports) and at the center (i.e., 5 ft from the supports). All string potentiometers were placed along the centerline of the specimen in the longitudinal direction.

Four concrete strain gauges measuring longitudinal strain were placed at the beam midspan. Two gauges were placed on the web and two were placed on the top and bottom flange of the beam to monitor the compressive and tensile strains along the beam height. Note that beam specimen L2 did not have longitudinal strain gauges on the web of the beam, only the top and bottom flange. Two strain gauge rosettes were placed on the web of the beam located approximately along the theoretical propagation of the shear cracking above the neutral axis at each end of the specimen. The rosettes measured the average strains in the web at 0°, 45°, and 90° at the location of the rosettes. These data were then used to calculate principal strains within the two critical locations on the beam. For concrete strain gauges to function properly, the sensors cannot be placed over any voids on the surface. Small voids (>0.125 in.) were filled with epoxy and sanded down so that only the strain in the concrete would control and be measured. Larger voids had to be avoided entirely. In the presence of large voids, the rosettes on each beam could not be placed in the exact same location and were shifted up to 2 in. in any direction while remaining as close as possible to the theoretical cracking path.

To measure the separation between the patch and the beam during loading, one horizontal and one vertical LVDT was placed on each patched section. Note that the beam specimen without patching did not have LVDT sensors. Instrumentation types and locations are shown in Figure 4.11.

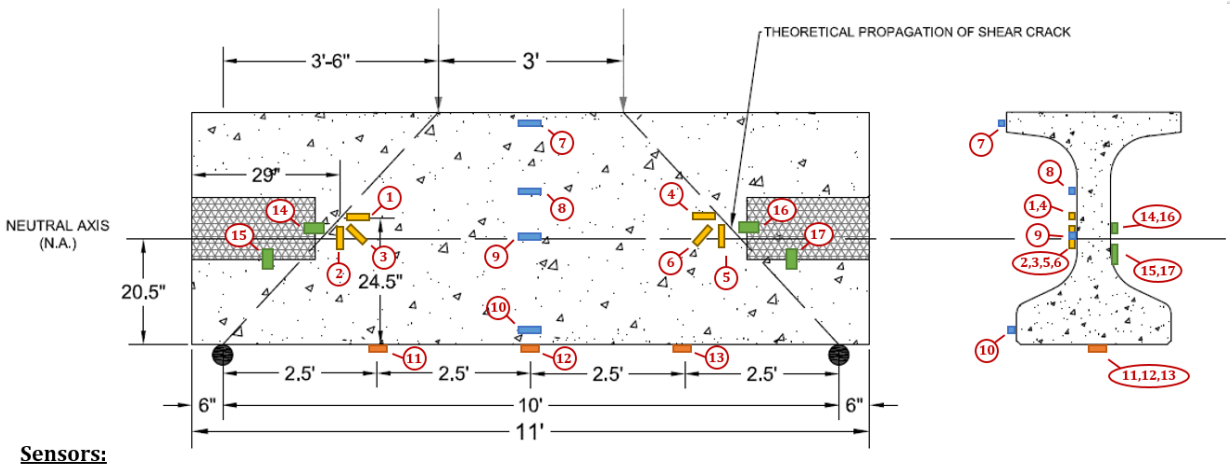

Sensors:

Strain Gauge Rosette	Longitudinal Strain Gauge	Displacement Gauge	LVDT
1 – NH – North Horizontal	7 – TF – Top Flange	11 – NDisp – North Displacement	14 – DNH – North Horizontal
2 – NV – North Vertical	8 – TW – Top Web	12 – MDisp – Middle Displacement	15 – DNV – North Vertical
3 – N45 – North 45°	9 – BW – Bottom Web	13 – SDisp – South Displacement	16 – DSH – South Horizontal
4 – SH – South Horizontal	10 – BF – Bottom Flange		17 – DSV – South Vertical
5 – SV – South Vertical			
6 – S45 – South 45°			

Figure 4.11. Beam instrumentation schematic

Results and Discussion

Cracking Behavior

The first sign of visible cracking in the Control-1 specimen occurred between 250 and 300 kips. Cracking propagated in the upper web at 35° from horizontal. Cracking occurred above the theoretical shear patch. Existing cracks that had formed due to cutting of the pretensioned steel cables expanded horizontally at loadings greater than 250 kips. Cracking propagated approximately 1 to 2 in. in each of the second and third load cycles, with little to no propagation in the final loading. The final crack pattern is shown in Figure 4.12.

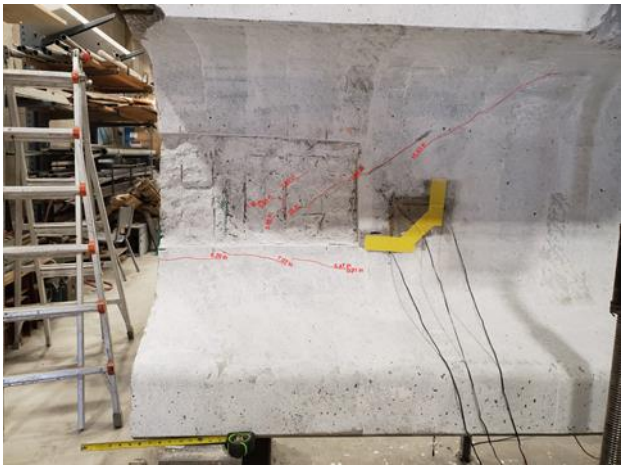

(a) Northwest

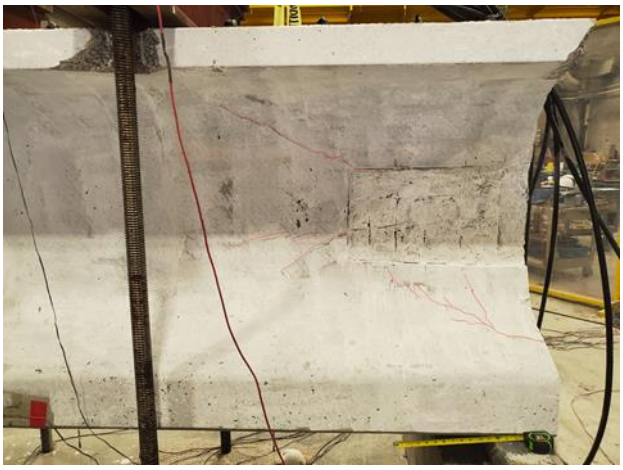

(b) Southwest

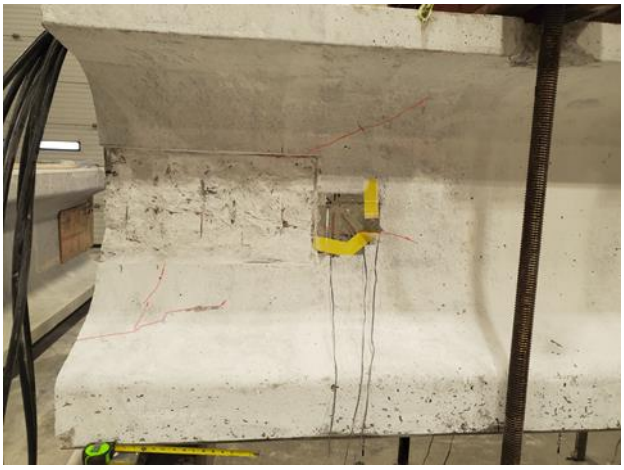

(c) Southeast

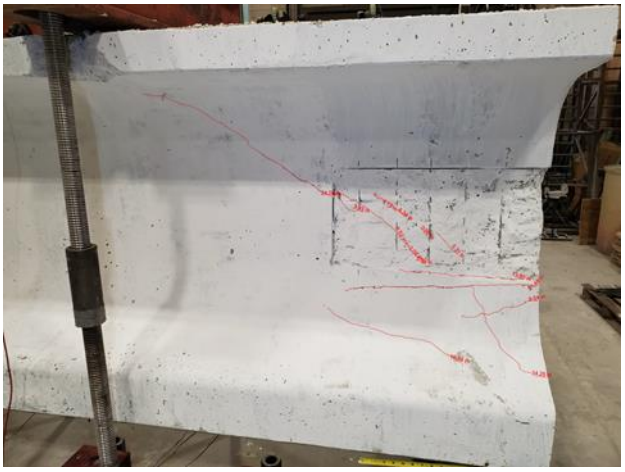

(d) Northeast

Figure 4.12. Crack pattern of Control-1

The Control-2 specimen was the only beam specimen to reach total failure. Significant shear cracking occurred in the web above the theoretical shear cracking path. The results of the initial loading had otherwise been comparable to those of other beam specimens. Cracking first occurred between 250 kips and 300 kips. During the second loading cycle, brittle failure occurred at a peak load of 400.6 kips (Figure 4.13).

Figure 4.13. Control-2 failure

The first stirrup from the south bearing fractured in one location: the bottom flange (Figure 4.14). Because of this, the mode of failure is assumed to be confinement failure, which caused the bottom flange to burst.

Figure 4.14. Fractured stirrup on bottom flange of Control-2

It should also be noted that the prestressed strands shrank approximately 1.25 in. into the beam following the bursting failure in the bottom flange. This indicates that there was prestressing

force remaining in the strands after the full-length beam was cut into the shorter test specimens (Figure 4.15).

Figure 4.15. South beam end of Control-2 after failure

The first sign of visible cracking in the UHPC-1 and UHPC-2 specimens occurred between 300 and 350 kips. Cracking started in the existing concrete outside of the repair region. Cracking propagated in the upper web at 40° from horizontal. Cracking occurred both above the theoretical shear path and along the expected path. Some existing cracks that had formed due to cutting of the pretensioned steel cables expanded horizontally at loadings greater than 300 kips. Cracking propagated approximately 1 to 2 in. in each of the second and third load cycles, with little to no propagation in the final loading. Visible cracking can be seen within the UHPC patching surface for both specimens, demonstrating an adequate bond between the patching material and the substrate (Figure 4.16 and Figure 4.17).

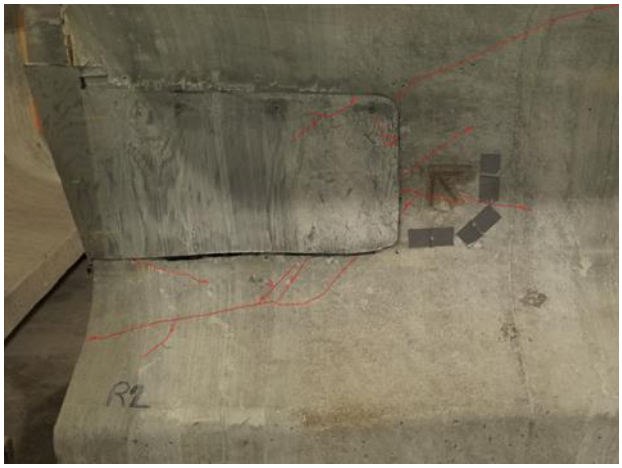

(a) Northwest

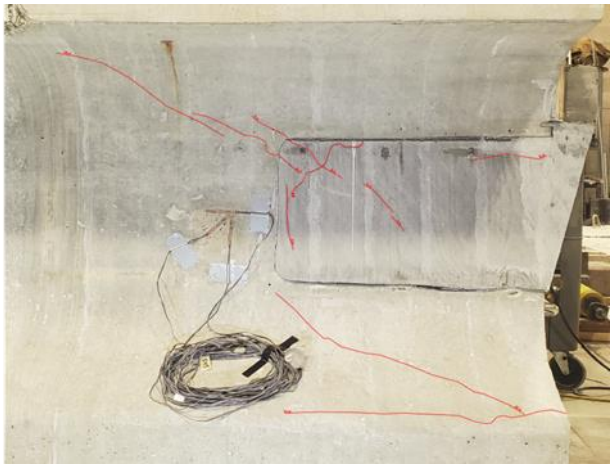

(b) Southwest

(c) Southeast

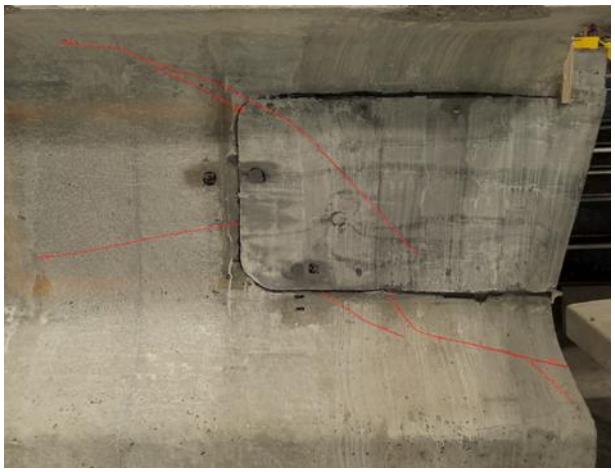

(d) Northeast

Figure 4.16. UHPC-1 crack pattern

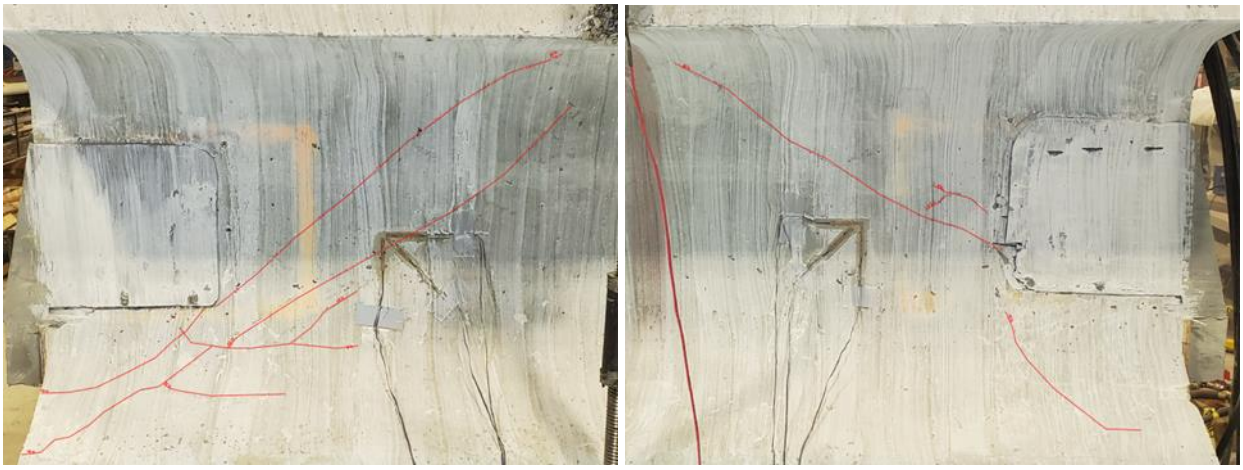

(a) Northwest (b) Southwest

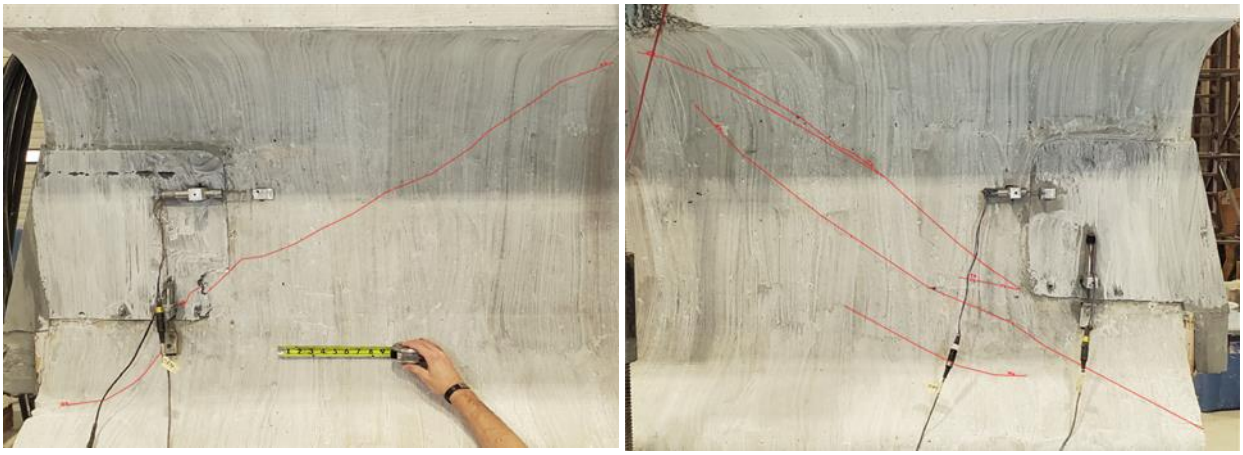

(c) Southeast (d) Northeast

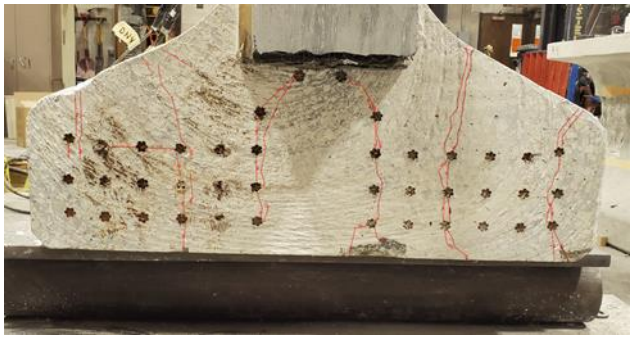

(e) Beam end

Figure 4.17. UHPC-2 crack pattern

Visible cracks appeared on the bottom flange of UHPC-2 at the interface of the NC and UHPC patch at loadings greater than 300 kips (Figure 4.18).

Figure 4.18. UHPC-2 south flange patch cracking along interface

The first sign of visible cracking in the HESC-1 and HESC-2 specimens occurred between 300 and 350 kips. Cracking started in the existing concrete outside of the repair region. Cracking propagated in the upper web at 45° from horizontal. Cracking occurred both above the theoretical shear path and along the expected path. Some existing cracks that had formed due to cutting of the pretensioned steel cables expanded horizontally at loadings greater than 300 kips. Cracking propagated approximately 1 to 2 in. in each of the second and third load cycles, with little to no propagation in the final loading. Visible cracking can be seen within the HESC patching surface for both specimens, demonstrating an adequate bond between the patching material and the substrate (Figure 4.19 and Figure 4.20). No visible cracks appeared on the bottom flange at the interface of the NC and HESC patch.

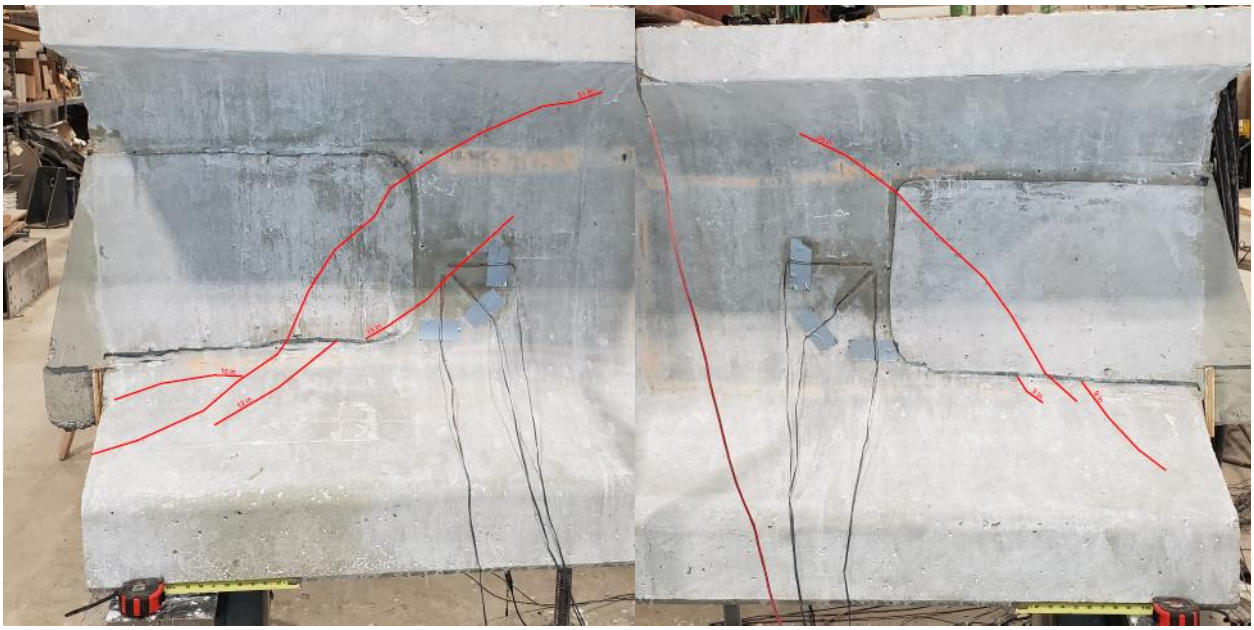

(a) Northwest (b) Southwest

(c) Southeast (d) Northeast

Figure 4.19. HESC-1 crack pattern

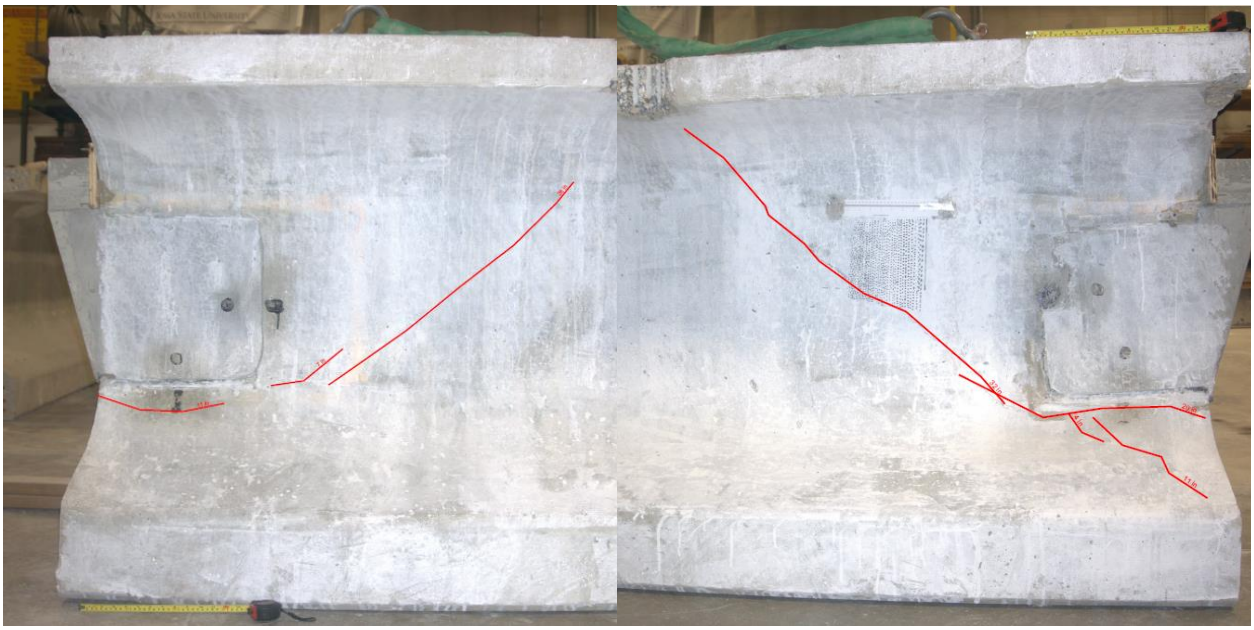

(a) Northwest (b) Southwest

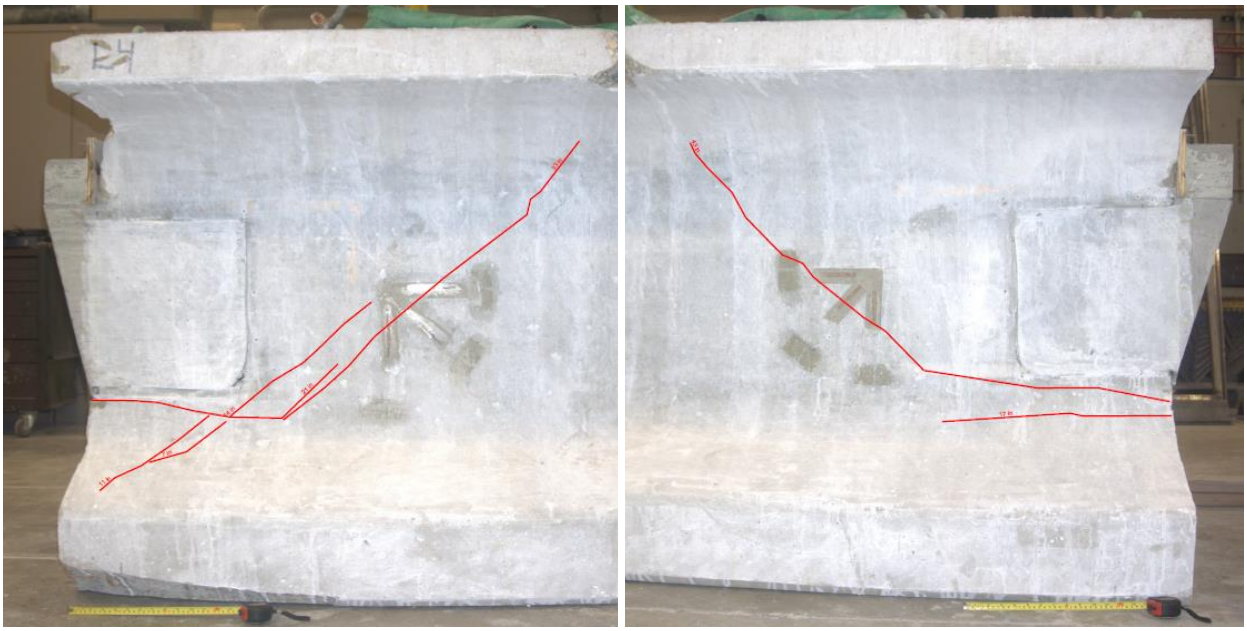

(c) Southeast (d) Northeast

Figure 4.20. HESC-2 crack pattern

Loads, Strains, and Deflections

Only one of the six beams (Control-2) reached failure during testing. Failure occurred during the second load cycle at a peak load of 400.6 kips. To allow a comparison of all of the beam specimens, the data presented in this section are from the first loading cycle. Cracking occurred in each of the tests during the first loading cycle, at which point some of the data recorded were no longer usable.

The maximum loads applied to the specimens are listed in Table 4.3.

Table 4.3. Maximum load for each specimen

Specimen	Max load (kips)
UHPC-1	421.9
UHPC-2	425.3
HESC-1	424.1
HESC-2	423.3
Control-1	429.2
Control-2	424.6

A plot of load versus midspan displacement for all specimens is depicted in Figure 4.21.

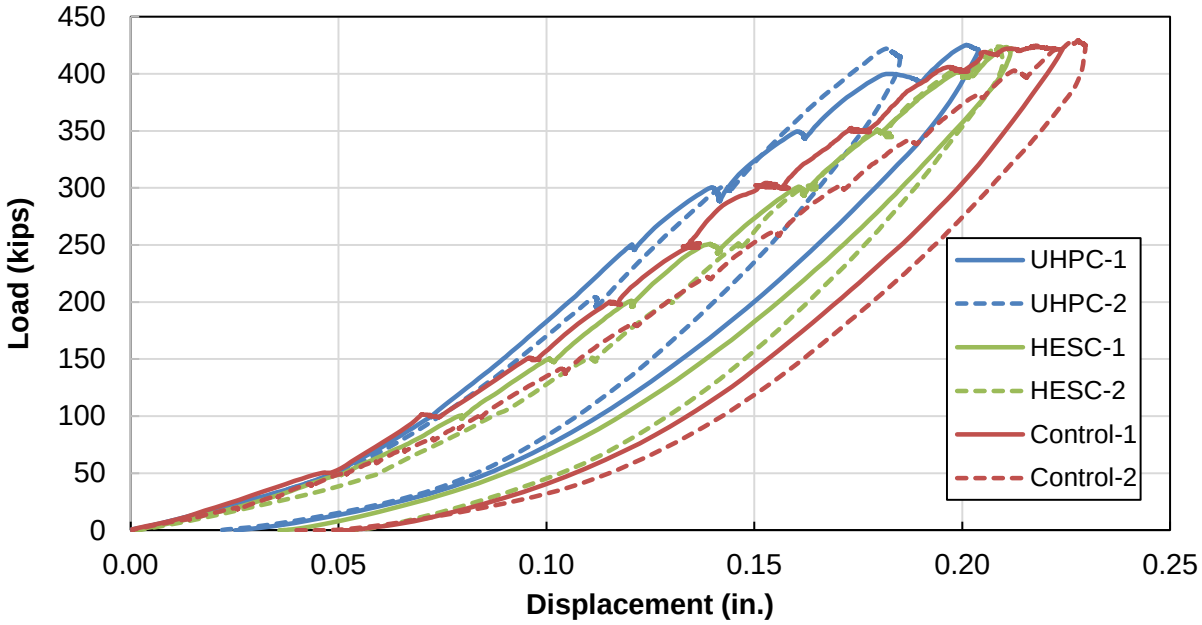

Figure 4.21. Load versus midspan displacement for all six specimens

For comparison, the midspan displacement values at a load of 421.9 kips are presented for all specimens in Table 4.4.

Table 4.4. Vertical deflection at midspan (in.)

UHPC-1	UHPC-2	HESC-1	HESC-2	Control-1	Control-2
0.182	0.199	0.207	0.210	0.224	0.215

From Figure 4.21 and Table 4.4, it can be seen that the beams that had undergone patching repair had lower deflections, with UHPC demonstrating the lowest values. However, given that the beam height is 45 in. and the maximum difference in total vertical displacement is less than 0.06 in., these results may not be considered significant.

While recording data for principal strain, multiple strain gauges within individual rosettes failed, resulting in inaccurate calculations. The results from those gauges were not included in the analysis comparing the different beams. Due to the variance in the exact location of each rosette on different beam specimens and the propagation of cracks through strain gauges during multiple tests, direct comparison is difficult. Table 4.5 shows the maximum and minimum strains experienced in each beam specimen at the location of the strain rosette.

Table 4.5. Principal strain

Beam	North		South	
specimen	Max	Min	Max	Min
UHPC-1	168	-673	--	--
UHPC-2	5,451	1,513	6,328	-1,292
HESC-1	390	-303	393	-592
HESC-2	7,283	-7,803	36,955	-20,942
Control-1	--	--	717	-496
Control-2	221	-519	272	-336

Note that any strain value surpassing -2,000 με represents cracked concrete. UHPC-2, HESC-2, and Control-2 all had a crack propagate through at least one strain gauge rosette during testing.

Displacement gauges placed on each patch were used to record the separation between the patch and the beam and thereby indicate when the patch delaminated from the beam. The displacement gauge readings shown in Table 4.6 are all below 0.01 in.

Table 4.6. Patch interface separation

	Sensor Location			
	North		South	
Specimen	Vertical (in.)	Horizontal (in.)	Vertical (in.)	Horizontal (in.)
UHPC-1	--	--	-0.0025	-0.0008
UHPC-2	-0.0037	-0.0003	-0.0008	-0.0020
HESC-1	-0.0031	--	-0.0026	-0.0007
HESC-2	-0.0029	--	-0.0004	--

The data recorded by the sensors used in this experiment do not overcome the bounds of error. This means that the beam web patches did not separate from the beam substrate. Both the UHPC and HESC patches demonstrated adequate bonding performance in full-scale testing.

Summary and Conclusions

- Upon completion of the monotonic loads, all of the repaired specimens maintained their integrity and performance with no failure. There were no significant differences observed in behavior under shear loading among the four patch-repaired girders in the large-scale study.

- The beams with patch repairs experienced lower maximum strains and deflections despite being subject to a greater maximum load, indicating that the patching exhibited good bond behavior during loading and unloading.

- Failure of one of the unrepaired beams due to confinement failure demonstrated one consequence of the loss of concrete cover caused by beam-end damage. Both the UHPC and HESC patches demonstrated good bonding to the beam substrate during full-scale testing. Patch repairs are significantly less expensive than beam replacement and are considered to be conventional bridge repairs.

- Further research on the practical aspects and strength-enhancing capabilities of UHPC and HESC for beam-end repair in shear-critical regions is recommended through field investigations.

SUMMARY AND CONCLUSIONS

Summary

In this study, the efficacy of UHPC and HESC for strengthening and repairing damaged prestressed concrete beam ends was evaluated. First, a review of current repair strategies was conducted to determine the key qualities of effective repair methods. The use of unique materials with enhanced properties to perform patch repairs was ultimately selected as the repair method evaluated in this research project. Small-scale laboratory testing was conducted to evaluate the bond strength of various potential patching materials in terms of shear stress and tensile stress. Full-scale laboratory testing was conducted to determine the properties and performance of UHPC and HESC as beam patching materials. Six artificially damaged prestressed concrete beams were tested in full-scale experiments: two without repair, two repaired with UHPC, and two repaired with HESC.

Observations indicated excellent patch bonding by the two materials tested in the full-scale portion of this research. Failure of one of the unrepaired beams (Control-1) due to confinement failure demonstrated one consequence of the loss of concrete cover and damage to the reinforcing steel caused by the beam-end damage.

Conclusions and Recommendations

The conclusions presented below were drawn from the small-scale testing of the bond strengths of various patching materials and the performance of repaired and unrepaired full-scale beam specimens.

The following conclusions were drawn from the small-scale investigation of bond strength:

- Small-scale bond testing for this project consisted of testing four different materials to determine their bonding properties and their suitability for use as patch repair materials. The materials tested included proprietary and nonproprietary UHPC, HESC, and SCC-C. Each material was tested under tensile stresses and shear stresses using the splitting tensile strength test and the slant shear strength test, respectively.

- All material types demonstrated satisfactory tensile bond strength. The interface surface condition did not demonstrate a significant effect on tensile bond strength for all samples. Both the HESC and SCC-C bonded samples exhibited a tensile bond strength exceeding the tensile strength of the plain (unbonded) samples tested. Both types of UHPC samples resulted in higher peak loads resisted. However, for all specimens, the substrate concrete failed before the testing machine reached peak load. Therefore, maximum tensile bond stress could not be determined.

- All of the tested material types demonstrated appropriate shear bond strength. No bond failures were observed during slant shear testing. In the case of the HESC and SCC-C

samples, failure initiated in the substrate concrete and cracking propagated as vertical splitting cracks in nearly all specimens. Pure substrate failure occurred for the UHPC samples. Some cracks penetrated the UHPC but were mitigated by the steel fibers in the mix. These results suggest that all of the identified materials provide adequate bond strength and are suitable for use as patch repair materials.

The following conclusions were drawn from the full-scale shear test of six beam specimens to investigate the efficacy of the patch repair method using different materials:

- Upon completion of the monotonic loads, all of the repaired specimens maintained their integrity and performance with no failure. There were no significant differences observed in behavior under shear loading among the four patch-repaired girders in the large-scale study.

- Failure of one of the unrepaired beams due to confinement failure demonstrated one consequence of the loss of concrete cover caused by corrosion damage. Both the UHPC and HESC patches demonstrated good bonding to the beam substrate during full-scale testing. Patch repairs are significantly less expensive than beam replacement and are considered to be conventional bridge repairs.

- The beams with patch repairs experienced lower maximum strains and deflections despite being subject to a greater maximum load, indicating that the patching exhibited good bond behavior during loading and unloading.

- Further research on the practical aspects and strength-enhancing capabilities of UHPC and HESC for beam-end repair in shear-critical regions is recommended through field investigations.

REFERENCES

ASTM C78/C78M-18. 2018. *Standard Test Method for Flexural Strength of Concrete (Using Simple Beam with Third-Point Loading)*. ASTM International, West Conshohocken, PA.

ASTM C882. 2015, 2018. *Standard Test Method for Bond Strength of Epoxy-Resin Systems Used with Concrete by Slant Shear*. ASTM International, West Conshohocken, PA.

ASTM C496/C496M-17. 2017. *Standard Test Method for Splitting Tensile Strength of Cylindrical Concrete Specimens*. ASTM International, West Conshohocken, PA.

ASTM C845/C845M-18. 2018. *Standard Specification for Expansive Hydraulic Cement*. ASTM International, West Conshohocken, PA.

ASTM C1583/C1583M-20. 2020. *Standard Test Method for Tensile Strength of Concrete Surfaces and the Bond Strength or Tensile Strength of Concrete Repair and Overlay Materials by Direct Tension (Pull-Off Method).* ASTM International, West Conshohocken, PA.

ASTM C1611. 2018. *Standard Test Method for Slump Flow of Self-Consolidating Concrete*. ASTM International, West Conshohocken, PA.

Bescher, E. P. 2018. *Calcium Sulfoaluminate-Belite Concrete: Structure, Properties, Practice*. Presentation. University of California Los Angeles, Los Angeles, CA. https://intrans.iastate.edu/app/uploads/2018/08/03-Wed-Bescher-Calcium-Sulfoaluminate-Belite-Concrete.pdf.

Carbonell Muñoz, M. A., D. K. Harris, T. M. Ahlborn, and D. C. Froster. 2014. Bond Performance between Ultrahigh-Performance Concrete and Normal-Strength Concrete. *Journal of Materials in Civil Engineering*, Vol. 26, No. 8.

Casanova, M., C. Clauson, A. Ebrahimpour, and M. Mashal. 2019. High-Early Strength Concrete with Polypropylene Fibers as Cost-Effective Alternative for Field-Cast Connections of Precast Elements in Accelerated Bridge Construction. *Journal of Materials in Civil Engineering*, Vol. 31, No. 11.

Chen, I. A., C. W. Hargis, and M. C. G. Juenger. 2012. Understanding Expansion in Calcium Sulfoaluminate-Belite Cements. *Cement and Concrete Research*, Vol. 42, No. 1, pp. 51–60.

Chen, W. F. and L. Duan, editors. 2014. *Bridge Engineering Handbook*. Taylor & Francis, Boca Raton, FL.

Clark, L.A. and B. S. Gill. 1985. Shear Strength of Smooth Unreinforced Construction Joints. *Magazine of Concrete Research*, Vol. 37, No. 131, pp. 95–100.

Clemena, G. C. and D. R. Jackson. 2000. *Trial Application of Electrochemical Chloride Extraction on Concrete Bridge Components in Virginia*. Virginia Transportation Research Council, Charlottesville, VA.

D'Antino, T., L. H. Sneed, C. Carloni, and C. Pellegrino. 2016. Effect of the Inherent Eccentricity in Single-Lap Direct-Shear Tests of PBO FRCM-Concrete Joints. *Composite Structures*, Vol. 142, pp. 117–129.

Dominguez Mayans, F. 2014. Analysis of a Damaged and Repaired Pre-Stressed Concrete Bridge Girder by Vehicle Impact and Effectiveness of Repair Procedure. Barcelona: Minor thesis. Construction Engineering Department, Barcelona School of Engineering, Spain.

ELTECH Research Corporation. 1993. *Cathodic Protection of Reinforced Concrete Bridge Elements: A State of the Art Report*. SHRP-S-337. Strategic Highway Research Program, Washington, DC. http://onlinepubs.trb.org/onlinepubs/shrp/SHRP-S-337.pdf.

Feldman, L. R., J. O. Jirsa, D. W. Fowler, and R. L. Carrasquillo. 1996. *Current Practice in the Repair of Prestressed Bridge Girders*. Center for Transportation Research, University of Texas at Austin, TX.

Ghafoori, N., M. Najimi, and M. Maler. 2017. *High-Early-Strength High-Performance Concrete for Rapid Pavement Repair*. SOLARIS Consortium, Center for Advanced Transportation Education and Research, University of Nevada Reno, NV.

Harries, K. A., J. Kasan, and J. Aktas. 2009. *Repair Method for Prestressed Girder Bridges*. University of Pittsburgh, PA.

Harris, D. M. Carbonell Munoz, A. Gheitasi, T. Ahlborn, and S. Rush. 2015. The Challenges Related to Interface Bond Characterization of Ultra-High-Performance Concrete with Implications for Bridge Rehabilitation Practices. *Advances in Civil Engineering Materials*, Vol. 4, No. 2, pp. 75–101.

Hasenkamp, C. J., S. S. Badie, C. Y. Tuan, and M. K. Tadros. 2008. Sources of End Zone Cracking of Pretensioned Concrete Girders. 2008 Concrete Bridge Conference, May 4–7, St. Louis, MO.

He, Y., X. Zhang, R. D. Hooton, and X. Zhang. 2017. Effects of Interface Roughness and Interface Adhesion on New-to-Old Concrete Bonding. *Construction and Building Materials*, Vol. 151, pp. 582–590.

Hosteng, T., A. Abu-Hawash, G. Port, and B. Phares. 2015. *Laboratory Investigation of Concrete Beam-End Treatments*. Bridge Engineering Center, Iowa State University, Ames, IA. https://intrans.iastate.edu/app/uploads/2018/03/beam-end_treatments_w_cvr.pdf.

Hussein, H. H., K. K. Walsh, S. M. Sargand, and E. P. Steinberg. 2016. Interfacial Properties of Ultrahigh-Performance Concrete and High-Strength Concrete Bridge Connections. *Journal of Materials in Civil Engineering*, Vol. 28, No. 5, pp. 1–10.

Iowa DOT. 2014. *Bridge Maintenance Manual*. Iowa Department of Transportation, Ames, IA.

Jafarinejad, S., A. Rabiee, and M. Shekarchi. 2019. Experimental Investigation on the Bond Strength between Ultra High Strength Fiber Reinforced Cementitious Mortar and Conventional Concrete. *Construction and Building Materials*, Vol. 229.

Júlio, E. N. B. S., F. A. Branco, and V. D. Silva. 2004. Concrete-to-Concrete Bond Strength. Influence of the Roughness of the Substrate Surface. *Construction and Building Materials*, Vol. 18, No. 9, pp. 675–681.

Kannel, J., C. E. French, and H. K. Stolarski. 1997. Release Methodology of Strands to Reduce t End Cracking in Pretensioned Concrete Girders. *PCI Journal*, Vol. 42, No. 1, pp. 42–54.

Karim, R., M. Najimi, and B. Shafei. 2019. Assessment of Transport Properties, Volume Stability, and Frost Resistance of Non-Proprietary Ultra-High Performance Concrete. *Construction and Building Materials*, Vol. 227.

Kasan, J. L., K. A. Harries, R. Miller, and R. J. Brinkman. 2014. Repair of Prestressed-Concrete Girders Combining Internal Strand Splicing and Externally Bonded CFRP Techniques. *Journal of Bridge Engineering*, Vol. 19, No. 2, pp. 200–209.

Kalfat, R., R. Al-Mahaidi, and S. T. Smith. 2013. Anchorage Devices Used to Improve the Performance of Reinforced Concrete Beams Retrofitted with FRP Composites: State-of-the-Art Review. *Journal of Composites for Construction*, Vol. 17, No. 1, pp. 14–33.

Kim, J.-m., H.-w. Kim, S.-y. Choi, and S.-y. Park. 2016. Measurement of Prestressing Force in Pretensioned UHPC Deck using a Fiber Optic FBG Sensor Embedded in a 7-Wire Strand. *Journal of Sensors*, Vol. 2016, pp. 1–9.

Liao, W., H. Wang, M. Li, C. Ma, and B. Wang. 2019. Large Scale Experimental Study on Bond Behavior between Polymer Modified Cement Mortar Layer and Concrete. *Construction and Building Materials*, Vol. 228.

Mather, B. 1970. *Expansive Cements*. U.S. Army Engineer Waterways Experiment Station, Vicksburg, MS.

Mindess, S., J. F. Young, and D. Darwin. 2002. *Concrete*, Second Edition. Prentice Hall, New York, NY.

Momayez, A., M. R. Eshani, A. A. Ramezanianpour, and H. Rajaie. 2005. Comparison of Methods for Evaluating Bond Strength Between Concrete Substrate and Repair Materials. *Cement and Concrete Research*, Vol. 35, No. 4, pp. 748–757.

Naderi, M. 2009. Analysis of the Slant Shear Test. *Journal of Adhesion Science and Technology*, Vol. 23, pp. 229–245.

Nawy, E. G. 2010. *Prestressed Concrete: A Fundamental Approach*, 3rd Edition. Prentice-Hall.

Needham, D. E. 2000. *Prestressed Concrete Beam End Repair*. Michigan Department of Transportation, Lansing, MI.

Nguyen, T. T. D., K. Matsumoto, A. Iwasaki, Y. Sato, and J. Niwa. 2013. Performance of Pretensioning Prestressed Concrete Beams with Ruptured Strands Flexurally Strengthened by CFRP Sheets. *Third International Conference on Sustainable Construction Materials and Technologies*, August 18–21, Kyoto, Japan. http://www.claisse.info/2013%20papers/data/e036.pdf.

Ohio DOT. 2007. *Abutments*. Ohio Department of Transportation, Columbus, OH.

Russell, H., R. Stadler, and H. Gelhardt, III. 2002. Shrinkage-Compensating Concrete Made with an Expansive Component. *Concrete International*, Vol. 24, No. 8, pp. 107–111.

Santos, P. M. D., E. B. S. Júlio, and V. D. Silva. 2007. Correlation between Concrete-to-Concrete Bond Strength and the Roughness of the Substrate Surface. *Construction and Building Materials*, Vol. 21, No. 8, pp. 1688–1695.

Shaw, I. and B. Andrawes. 2017. Repair of Damaged End Regions of PC Beams using Externally Bonded FRP Shear Reinforcement. *Construction and Building Materials*, Vol. 148, pp. 184–194.

Shi, C., Z. Wu, J. Xiao, D. Wang, Z. Huang, and Z. Fang. 2015. A Review on Ultra-High Performance Concrete: Part I. Raw Materials and Mixture Design. *Construction and Building Materials*, Vol. 101, Part 1, pp. 741–751.

Shield, C. and P. Bergson. 2018. *Experimental Shear Capacity Comparison Between Repaired and Unrepaired Girder Ends*. Minnesota Department of Transportation, St. Paul, MN.

Silfwerbrand, J. 2003. Shear Bond Strength in Repaired Concrete Structures. *Materials and Structures*, Vol. 36, pp. 419–424.

Tadros, M. K., S. S. Badie, and C. Y. Tuan. 2010. *NCHRP Report 654: Evaluation and Repair Procedures for Precast/Prestressed Concrete Girders with Longitudinal Cracking in the Web*. National Cooperative Highway Research Program, Washington, DC.

WisDOT. 2017. *WisDOT Bridge Manual*, Chapter 10 - Prestressed Concrete. Wisconsin Department of Transportation, Madison, WI.

Wu, N. C. and S. Chase. 2010. *An Exploratory Data Analysis of National Bridge Inventory*. Mid-Atlantic Universities Transportation Center, Pennsylvania State University, State College, PA.
Zanotti, C. and N. Randl. 2019. Are Concrete-Concrete Bond Tests Comparable? *Cement and Concrete Composites*, Vol. 99, pp. 80–88.

THE INSTITUTE FOR TRANSPORTATION IS THE FOCAL POINT FOR TRANSPORTATION AT IOWA STATE UNIVERSITY.

InTrans centers and programs perform transportation research and provide technology transfer services for government agencies and private companies;

InTrans contributes to Iowa State University and the College of Engineering's educational programs for transportation students and provides K–12 outreach; and

InTrans conducts local, regional, and national transportation services and continuing education programs.

IOWA STATE UNIVERSITY

Visit **InTrans.iastate.edu** for color pdfs of this and other research reports.